Journal of Materials Chemistry A

REVIEW

View Article Online
View Journal | View Issue

Cite this: J. Mater. Chem. A, 2023, 11, 13844

Multifunctional small biomolecules as key building blocks in the development of hydrogel-based strain sensors

Syed Farrukh Alam Zaidi, [ab] Aiman Saeed, [c] Jun Hyuk Heo [*ad] and Jung Heon Lee [*ade]

Received 17th March 2023
Accepted 16th May 2023

DOI: 10.1039/d3ta01627g

rsc.li/materials-a

Hydrogels are three-dimensional polymer networks that are considered a promising option for developing strain sensors due to their stretchability, mechanical robustness, and high water content. These attributes make hydrogel-based sensors suitable for various applications, such as wearable electronics, human–machine interfaces, health monitoring, and soft robotics. Small biomolecules, which are biologically derived and possess attributes such as renewability, eco-friendliness, and multifunctionality, have been consistently explored for use in hydrogel-based strain sensors to improve their multifunctional properties and strain-sensing performance. This review offers a comprehensive overview of incorporating small biomolecules in developing hydrogel-based strain sensors, with a focus on enhancing their multifunctional properties and strain-sensing performance. Firstly, the representative applications and strain-sensing mechanisms of hydrogel-based strain sensors are introduced. Subsequently, the status of the functional properties of the hydrogels and the performance indicators of their strain-sensing abilities are outlined. Finally, multifunctional small biomolecules are described, followed by a comprehensive discussion concerning recent developments regarding their role in enhancing various functional properties and the performance of hydrogel-based strain sensors. Furthermore, the latest trends and perspectives on the future of hydrogel-based strain sensors are also reported.

[a]School of Advanced Materials Science and Engineering, Sungkyunkwan University (SKKU), Suwon 16419, Republic of Korea. E-mail: jhlee7@skku.edu; Fax: +82-502-302-1918; Tel: +82-31-290-7404

[b]Department of Metallurgical and Materials Engineering, University of Engineering and Technology (UET), Lahore 54890, Pakistan

[c]Department of Biomedical Engineering, Sungkyunkwan University (SKKU), Suwon 16419, Republic of Korea

[d]Research Center for Advanced Materials Technology, Core Research Institute, Suwon 16419, Republic of Korea

[e]Biomedical Institute for Convergence at SKKU (BICS), Sungkyunkwan University (SKKU), Suwon 16419, Republic of Korea

Syed Farrukh Alam Zaidi obtained his BSc (2014) and MSc (2017) degrees in Metallurgical and Materials Engineering from the University of Engineering and Technology, Lahore, Pakistan. He is presently pursuing his PhD in the School of Advanced Materials Science and Engineering at Sungkyunkwan University, South Korea. Syed's research primarily focuses on the innovation of biomolecule-based conductive hydrogels, with applications in sensors and energy storage devices.

Aiman Saeed earned her BSc (2020) in Biomedical Engineering from the NED University of Engineering and Technology, Karachi, Pakistan. She is currently pursuing her MSc in the Department of Biomedical Engineering at Sungkyunkwan University in South Korea. Aiman's research interests focus on the development of biomolecule-based conductive hydrogels, targeting applications in sensors and energy storage devices.

Introduction

Strain sensors are used in various applications such as human–machine interfaces, robotic smart skins, health care monitoring, and bio-integrated devices.[1,2] Paper-based strain sensors can be classified into three types based on their working modes: bending,[3,4] pressure,[5,6] and tensile[7,8] sensors. However, only bending and pressure sensors are typically considered for flexible paper-based strain sensors due to the limited stretchable properties of paper,[4,9,10] which limit the potential of sensing to only small strain ranges.

Stretchable hydrogels are currently in the spotlight as strain sensors for flexible and wearable electronic devices, showing promise for detecting a wide range of strains, which increases the versatility of sensors for various applications.[11–13] Typically, hydrogels are formed by two different methods: three-dimensional polymerization (in which hydrophilic monomers are polymerized with cross-linking polyfunctional reagents) and cross-linking with water-soluble polymers.[14–17] However, these methods often produce a significant amount of residual monomers, resulting in toxicity issues of hydrogels.[18,19] Notably, the residual monomers were purified by extraction in excess water for several weeks.[14] Moreover, imparting multiple functions to hydrogels typically involves complex and multistep procedures, which can impede the practical adoption of hydrogels as platforms for strain sensors.[20–23] In addition, most ingredient molecules are synthetic and non-renewable and do not support green fabrication technology as a sustainable development approach.[24–27] Therefore, to support sustainable development, alternative molecules must be used to suppress toxicity and provide green fabrication processes for hydrogel strain sensors. Small biomolecules are a favored choice in this regard.

Small biomolecules are organic molecules produced in living organisms. They are essential because they are crucial in maintaining important physical and biological functions in living organisms.[28–30] For example, tannic acid (TA) is a polyphenolic compound containing multiple hydroxyl (–OH) and carboxyl (–COOH) groups that confer polyacid properties.[31] It is found in various plant sources, including tea, wine, and oak wood, and is commonly used as a food additive in various industrial applications.[32] It participates in defense mechanisms against parasites and oxidative stress[33,34] and regulates the reproductive system[35] and nutrient storage[36] in plants. The fascinating influence of small biomolecules has spurred the need to review their role in producing hydrogel strain sensors with various advantageous characteristics. This review focuses on various biomolecules and highlights how they impart important functional properties to hydrogels for strain sensors, such as mechanical toughness, stretchability, self-healing, self-adhesion, reusability, freezing tolerance, dehydration resistance, ultraviolet (UV) blocking, electrical conductivity, antibacterial properties, and biocompatibility. The latest trends and perspectives on the future of this field are also presented.

Advantages of small biomolecules in hydrogels

In particular, small biomolecules have critical advantages for hydrogel strain sensors, such as biocompatibility, functionality, and ease of fabrication. This may lead to the development of advanced hydrogels with excellent functionality for hydrogel strain sensors.[37] For example, several studies have shown that as a natural source, TA tunes the biological behavior of hydrogels in various fields, including strain sensors, enhancing their biocompatibility, biodegradability, and antibacterial and adhesion properties (Fig. 1). Sahiner *et al.* reported a TA-based hydrogel film that exhibited biocompatibility and biodegradability as a potential wound-healing dressing[38] (see Fig. 1(a) and (b)). In addition, TA helps form supramolecular hydrogels through complexation with trivalent cations, such as ferric ions (Fe^{3+}) (see Fig. 1(c)). Fan *et al.* demonstrated a supramolecular

Jun Hyuk Heo received his BS (2013) and PhD (2018) from the School of Advanced Material Science and Engineering, Sungkyunkwan University, South Korea. After working at Lotte Chemical as a senior researcher, he joined the Research Center for Advanced Materials Technology, Sungkyunkwan University, as a research professor. He also worked as a marketing director for NucleoEX corporation. His research interests include the development of smart sensors for ecosystem monitoring, bio-inspired eco-friendly materials, and bio-derived flame-retardant materials.

Jung Heon Lee is an Associate Professor at the School of Advanced Materials Science and Engineering at SKKU. He received his BS, MS, and PhD degrees in Materials Science and Engineering from Yonsei University, Seoul National University, and University of Illinois at Urbana-Champaign. Dr Lee's research is focused on developing nanoscale materials or devices that can be applied to diverse levels of biological systems for diagnostics or therapeutics. He also investigates strategies for exploiting the tunable properties of bio-derived materials toward the fabrication of smart materials or advanced nanoscale devices, including multifunctional hydrogel-based materials and sensors.

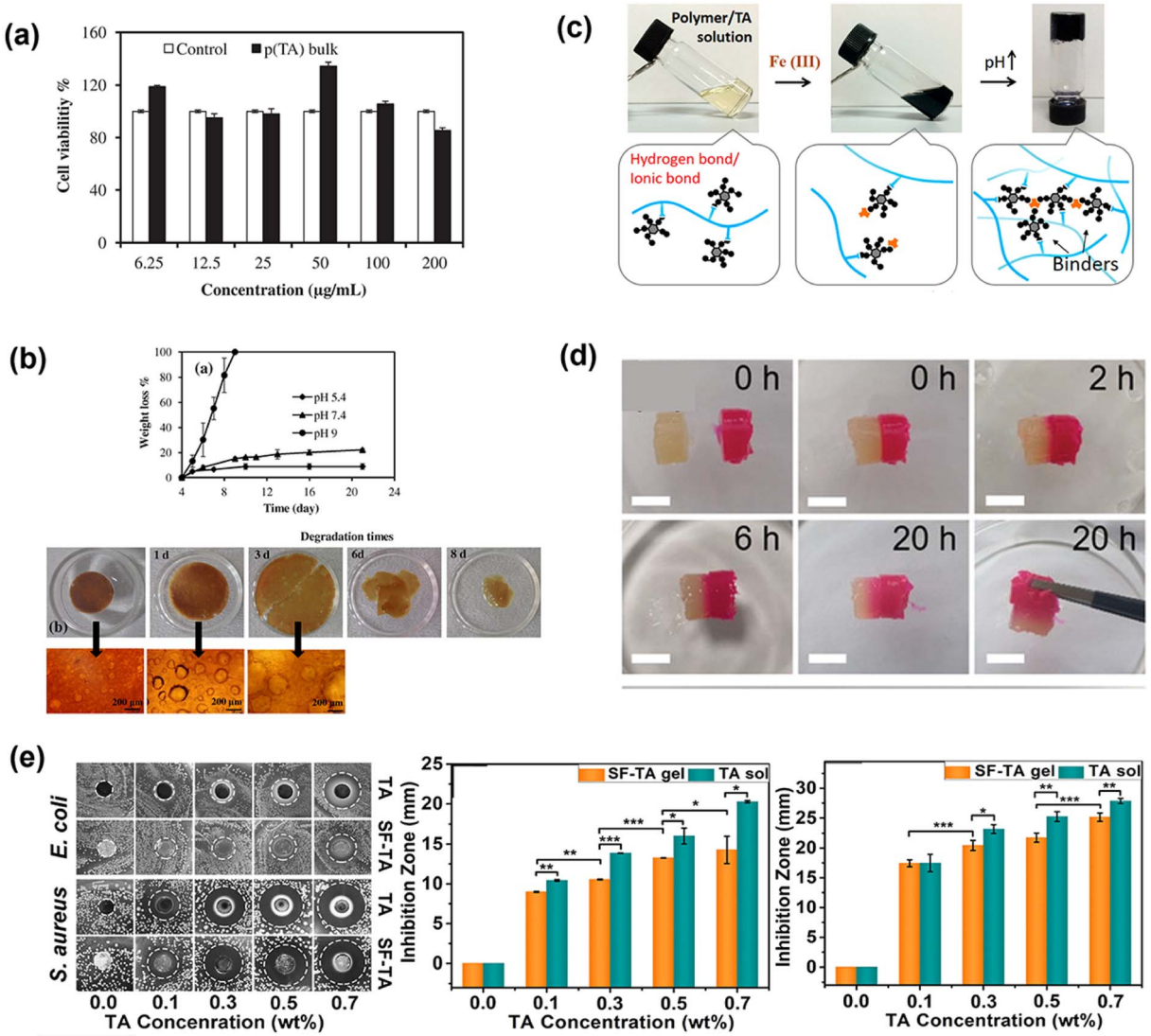

Fig. 1 (a) Cell viability of a tannic acid (TA)-based hydrogel with different concentrations of hydrogel extracts ranging from 6.25 to 200 μg mL^{-1} and (b) biodegradability of the TA-based hydrogel in various pH media over time.[38] Copyright 2015, Elsevier. (c) TA as a building block of a supramolecular hydrogel.[39] Copyright 2017, American Chemical Society. (d) Self-healing properties of a TA-containing 4-formylbenzoic acid hydrogel.[40] Copyright 2021, John Wiley and Sons. (e) Antibacterial properties of a silk fibroin (SF)-based hydrogel against *S. aureus* and *E. coli* bacteria with different contents of TA.[41] Copyright 2019, American Chemical Society.

TA-based hydrogel with multiple properties such as mechanical stability, quick self-repair, pH-stimuli responsiveness, and free radical scavenging capacity.[39] TA also exhibits self-healing properties in hydrogels owing to its dynamic chemical interactions with polymer networks[40] (see Fig. 1(d)). Furthermore, the addition of TA effectively induced the gelation of silk fibroin, creating a hybrid hydrogel with good antibacterial properties.[41] The increased TA content in the hydrogel improved antibacterial properties, increasing the inhibition zone of bacterial growth (see Fig. 1(e)). Finally, biomolecules are considered renewable and environmentally friendly because they can be produced through biological processes, such as fermentation or extraction from natural sources. They support green production technology because they can be manufactured on a large scale without needing nonrenewable resources or toxic chemicals, which can reduce production costs.[24]

Multifunctionality of small biomolecules in hydrogel-based strain sensors

The integration of small biomolecules provides several benefits for the advancement of hydrogel-based strain sensors with multiple functionalities. Hydrogel networks are primarily composed of either natural or synthetic polymers, which have limited ability to provide multifunctionality in their native form. Conversely, multifunctionalities are essential for expanding the practical applications of hydrogel-based strain sensors. For example, hydrogels must exhibit electrical conductivity to be effective as piezoresistive strain sensors. Polyelectrolytes such as sodium alginate can help create hydrogel networks and provide electrical conductivity. However,

they lack important characteristics such as resistance to dehydration and freezing.[42,43] Small ionizable biomolecules, such as phytic acid (PA), can be introduced into hydrogel networks based on polyelectrolytes to address these shortcomings. These biomolecules offer good electrical conductivity and can withstand freezing and dehydration.[44,45] Although natural polymers such as gelatin lack self-healing properties,[46–50] introducing TA facilitates excellent multifunctionality, including tunable mechanical strength and self-healing, in gelatin hydrogels.[51–53] Similarly, although alginate and chitosan (CS) are excellent natural polymers for hydrogel formation, they lack self-healing and adhesive capabilities in their native form. Inducing self-healing and adhesive properties requires laborious and time-consuming procedures,[20–22] which can impede the practical adoption of hydrogels for fabricating strain sensors. However, sodium alginate- and CS-based hydrogels prepared *via* a simple one-pot method with the addition of TA provide a much more accessible approach for adaptable structures, as TA is rich in functional groups, which can provide crosslinking to form hydrogels with self-healing and adhesion properties.[42,54] Additionally, while the polymer networks of hydrogels are not inherently UV-blocking, the integration of TA can provide multifunctionalities, such as tunable mechanical strength, self-healing, adhesion, bacterial resistance, and UV-blocking capabilities.[55,56] Furthermore, incorporating small biomolecules such as zwitterionic osmolytes,[57] sorbitol,[58] and PA[44,45] can offer a great opportunity to provide hydrogels with multifunctional properties, including the ability to withstand freezing temperatures and the capacity to adjust their mechanical properties. Based on this discussion and the general benefits of using small biomolecules in hydrogels, the merits of using small biomolecules to develop hydrogel-based strain sensors are summarized in Fig. 2.

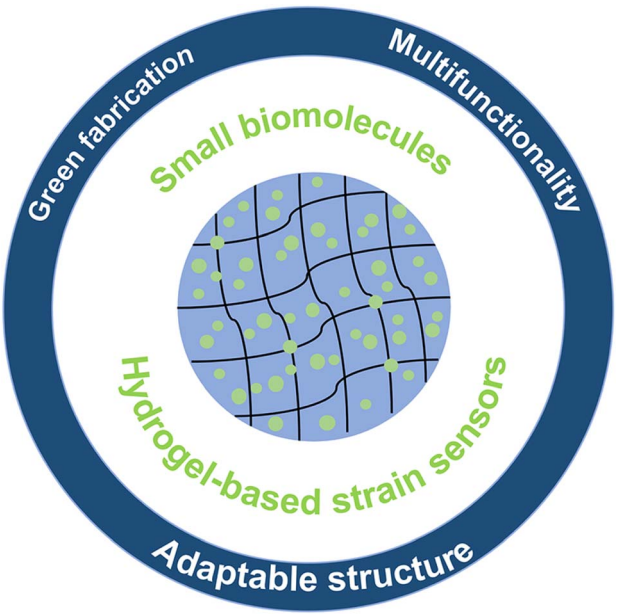

Fig. 2 Benefits of small biomolecules in developing hydrogel-based strain sensors.

Applications and sensing mechanisms of hydrogel-based strain sensors

Applications

Hydrogels have attracted attention as strain sensors in human health and physiological signal monitoring,[59,60] soft robotics,[61,62] and human–machine interfaces.[63–65] Hydrogel strain sensors have recently been applied as wearable sensors in wrist pulse or heart rhythm monitors,[66,67] visual sensors,[68,69] and human interaction[70] and motion monitors.[71,72] Furthermore, hydrogel-based implantable sensors have been used to monitor organ movements[73] and activity[74] (Fig. 3).

Hydrogel-based strain sensors, such as electronic skins, are a type of artificial intelligent skin that offers various benefits, including softness, high stretch/toughness, and high water content.[78,79] These sensors can be used in artificial skin for automation and human–machine interaction, which involves the development of software, hardware, and systems to improve communication between humans and computers. This can include features such as graphical user interfaces, voice recognition, and gesture-based input, enhancing the user experience and productivity (Fig. 4).

Mechanisms of strain sensing

Strain sensors can be classified into different types based on their sensing mechanism: piezoresistive, capacitive, piezoelectric, triboelectric, or dual mode,[76,82–84] as shown in Fig. 5. Each type converts the physical deformation into a change in the electronic signal.

Piezoresistive hydrogel strain sensors. When a hydrogel strain sensor is subjected to mechanical stress, the hydrogel deforms, causing a change in the distance and orientation of the conductive particles or ions. This change resulted in a variation in the electrical resistance (R), as shown in Fig. 5(a), indicated by the glow of the blue LED in Fig. 6(B). A piezoresistive strain-sensing mechanism was demonstrated using the conductive hydrogels. The conductivity of the hydrogels can be categorized into: (1) polymer-based conductivity, which is obtained from hydrogel networks made of conducting polymers such as polyaniline[86] and polypyrrole;[87,88] (2) conductivity based on fillers, such as carbon nanotubes,[89] graphene,[90] MXene sheets,[91] liquid metal,[71,92] Ag nanoparticles (AgNPs),[93] and wires;[48] (3) conductivity based on ions including inorganic salt ions (sodium citrate[46] and sodium chloride[94,95]) and organic salt ions (lignosulfonate[96]), as shown in Fig. 6(A). The percentage of relative change in the electrical resistance was plotted against the percentage of mechanical strain, and the resulting slope of the plot provides the strain sensitivity, also known as the Gauge Factor (GF), of the piezoresistive strain sensor (see Fig. 6(C)).

Capacitive hydrogel strain sensors. The capacitive hydrogel strain sensor converts the mechanical strain on its surface into a change in capacitance (C), as shown in Fig. 5(b) and 7(a). The capacitive strain sensor comprised two electrodes made of a conductive hydrogel sandwiched between dielectric materials. When the sensor is subjected to strain, the distance between the electrodes changes, resulting in a variation in the

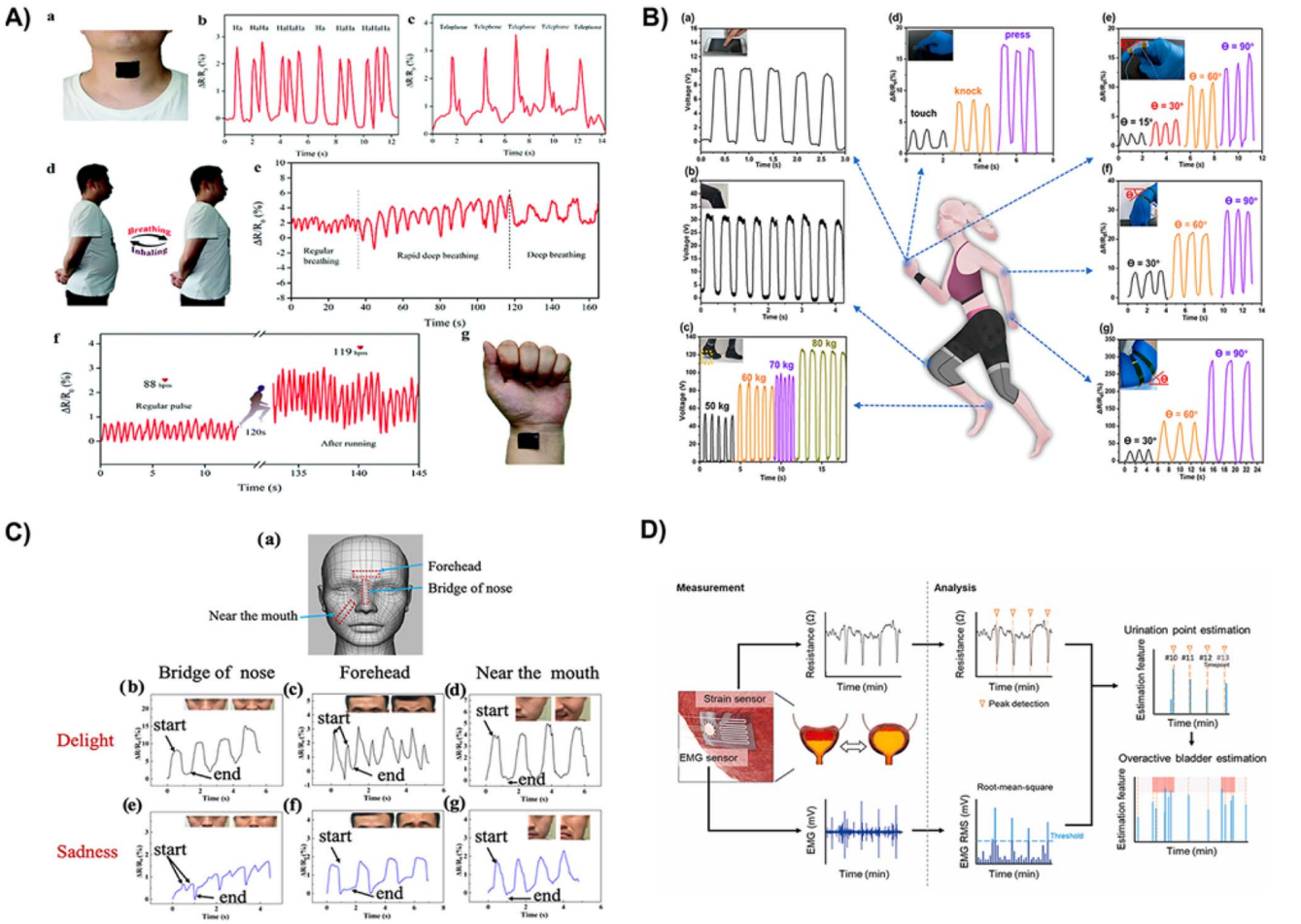

Fig. 3 Application of hydrogel-based strain sensors in real-time human motion and physiological signal monitoring. (A) Monitoring of small-scale motions such as laughing, speaking, breathing, and pulse detection (based on ref. 75). Copyright 2019, Royal Society of Chemistry. (B) Monitoring of large-scale motions of body parts, including finger compression, knee, wrist and elbow movements, and distinguishing the weights. Adapted with permission from ref. 76. Copyright 2022, American Chemical Society. (C) Detection of human emotions, including delight and sadness. With permission from ref. 70. Copyright 2020, American Chemical Society. (D) Implantable hydrogel-based strain sensor to monitor the activity of the bladder. Reproduced with permission from ref. 77. Copyright 2023, Elsevier.

capacitance.[99,100] The sensitivity of the capacitive hydrogel strain sensor was determined from the slope of the percentage change in the capacitive reactance *versus* the percentage mechanical strain plot.

Piezoelectric hydrogel strain sensors. Piezoelectric hydrogel strain sensors can directly convert mechanical energy, strain, or stress into electrical voltage (V) signals, making them useful as both strain sensors and generators,[85] as shown in Fig. 5(c). This conversion occurs because of the separation of charged centers within the piezoelectric material, such as lead zirconate titanate (PZT),[101] barium titanate ($BaTiO_3$ or BTO),[76] and poly(vinylidene fluoride-*co*-trifluoroethylene) or PVDF-TrFE[83] upon undergoing deformation, which generates an electrostatic potential that produces positive and negative charges on the surface of the device or electrodes. This process is illustrated in Fig. 8(a) and (b). The magnitude of the strain or force is directly correlated with the quantity of accumulated charges (Fig. 8(c) and (d)). Consequently, the mechanical signals are transformed into electrical signals, as shown in Fig. 8(e). The piezoelectric hydrogel can monitor low pressure, distinguish weight, and identify walking posture in real-time. The sensor can measure the open-circuit voltage between the human body and the ground to detect finger sliding on mobile phones and knee movement, distinguishing the different weights of student volunteers (Fig. 8(f–h)).

Triboelectric hydrogel strain sensors. Triboelectric hydrogel strain sensors utilize the triboelectric effect to convert mechanical strain or pressure into electrical signals. The sensor comprises two thin layers of different materials separated by a small gap, generating an electric charge when subjected to a strain or pressure,[102–105] as shown in Fig. 5(d), 9(a) and (c). The electrodes on the sensor surface detect the charge and produce an electrical signal in response to the magnitude of the strain, which can be amplified and processed (see Fig. 9(g)). The triboelectric generator made of E_{coflex} and polyvinyl alcohol (PVA)/poly(acrylamide-*co*-acrylic acid)-Fe^{3+} double-network hydrogel electrodes exhibited high adhesive stability under deformation (Fig. 9(b)), ensuring continuous electrical output. The device generates electricity through the contact and separation motions of the friction layers, resulting in the transfer of excess cations

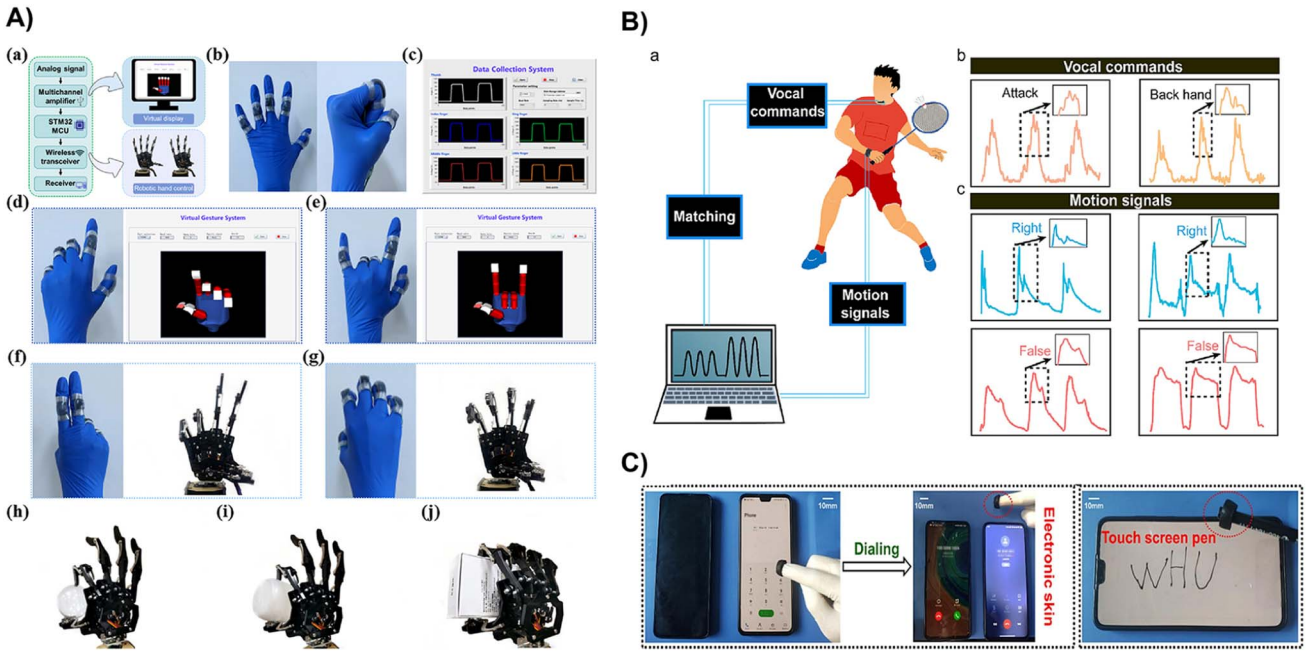

Fig. 4 Application of hydrogel-based strain sensors in artificial skins and human–machine interaction. (A) Gesture-based intelligent recognition system utilizing object-machine interaction (based on ref. 65). Copyright 2023, American Chemical Society. (B) Real-time monitoring of voice commands and motion signals *via* human–machine interaction. Adapted with permission from ref. 80. Copyright 2023, Elsevier. (C) Dialing on a cell phone and touching the phone screen using artificial skin. With permission from ref. 81. Copyright 2022, Elsevier.

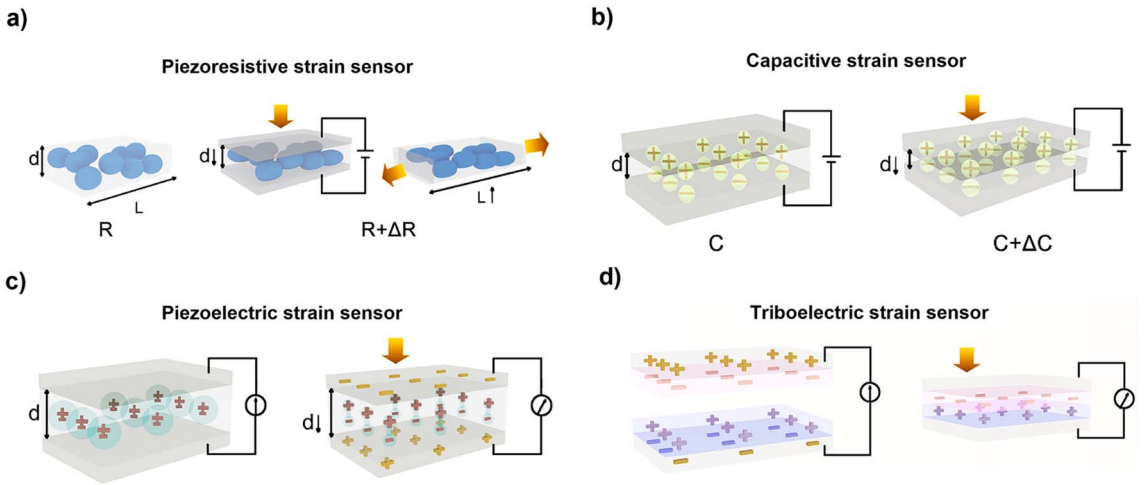

Fig. 5 Various operating principles of flexible strain sensors. (a) Piezoresistive strain sensor. (b) Capacitive strain sensor. (c) Piezoelectric strain sensor. (d) Triboelectric strain sensor (based on ref. 85). Copyright 2022, Elsevier.

and negative ions (Fig. 9(c)). The triboelectric hydrogel-based generator had a maximum open-circuit voltage (V_{oc}) of 238 V (Fig. 9(d)), short-circuit current (I_{sc}) of 1.2 μA (Fig. 9(e)), and short-circuit transferred charge (Q_{sc}) of 37 nC (Fig. 9(f)). Increasing the strain from 0 to 160% led to a significant increase in the V_{oc} of the triboelectric hydrogel-based generator (Fig. 9(g)), indicating the potential of the device as a strain sensor. A triboelectric generator device can monitor human motion (Fig. 9(h)).

Dual mode hydrogel strain sensors. Recent progress in the design of hydrogel-based strain sensors has enabled the development of dual-mode strain-sensing mechanisms for multiple applications, such as combining piezoresistive and piezoelectric properties,[83,106] piezoresistive and triboelectric properties,[82,100] or piezoresistive and capacitive properties.[69,100,107] For example, a dual-mode mechanism comprising piezoresistive and piezoelectric properties can be achieved by incorporating the piezoelectric material PVDF-TrFE into a conductive hydrogel network.[83,106] Similarly, other combinations of sensing mechanisms can be realized by altering the device assembly while preparing the application-mechanism-oriented hydrogel composition.

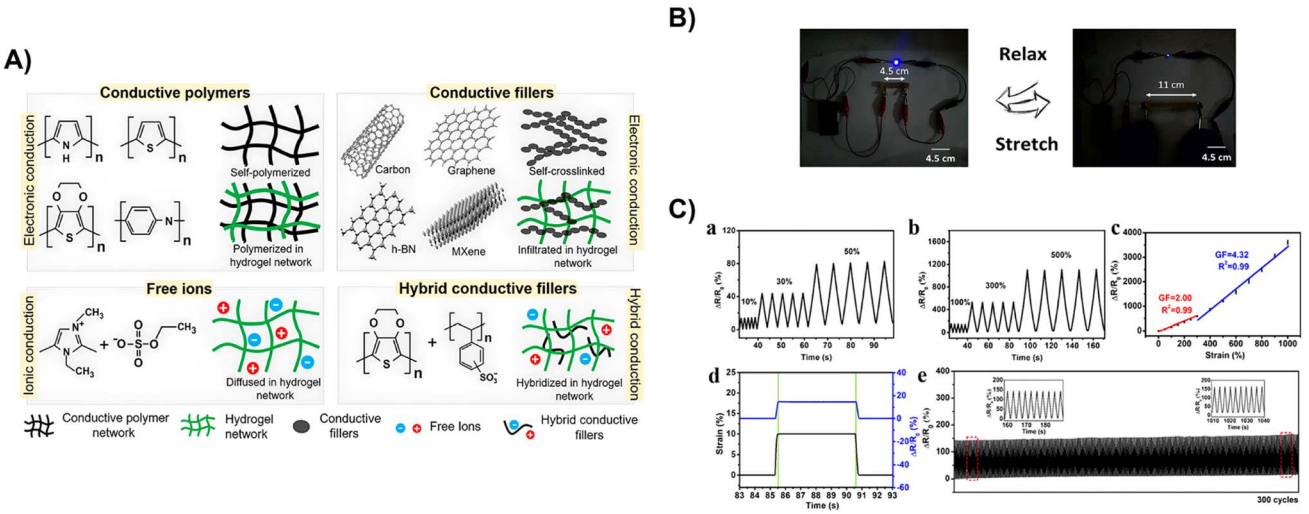

Fig. 6 (A) Various modes of electrical conductivity in conductive hydrogels.[97] Copyright 2020, American Chemical Society. (B) The figure depicts the effect of stretching and relaxing a hydrogel-based strain sensor, with resistance changes visualized under blue LED illumination (adapted from ref. 51). Copyright 2022, Elsevier. (C) Performance of a piezoresistive hydrogel strain sensor.[98] Relative change of resistance ($\Delta R/R_0$) under cyclic stretching–releasing at (a) low mechanical strains and (b) high mechanical strains. (c) $\Delta R/R_0$ with various strains applied up to 1000% and resulting GFs. (d) Strain change and $\Delta R/R_0$ curves of the strain sensor under instantaneous stretching–relaxing for 10% strain. (e) The durability of hydrogel strain sensors at a strain of 100% for 300 cycles. Adapted with permission from ref. 98. Copyright 2020, American Chemical Society.

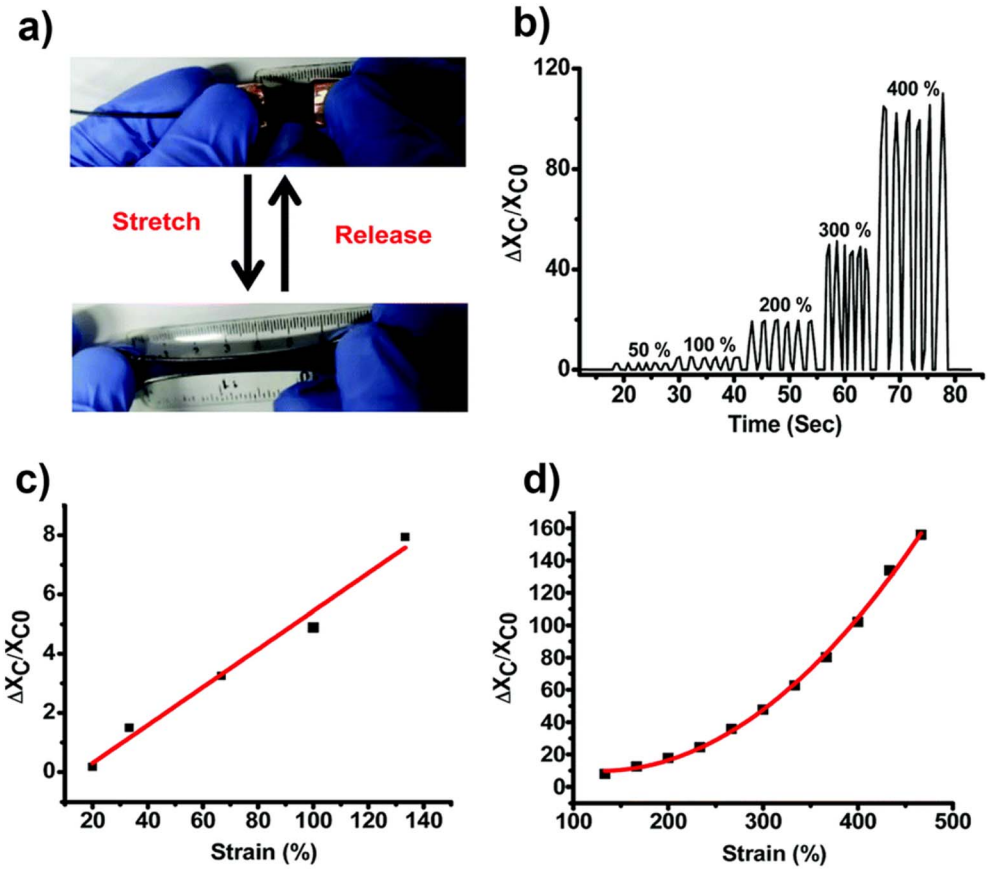

Fig. 7 Performance of the capacitive hydrogel strain sensor.[99] (a) Picture of the stretch/release cycle. (b) Change in capacitive reactance ($\Delta X_C/X_{C0}$) upon stretching/releasing at various strain magnitudes from 50 to 400%. $\Delta X_C/X_{C0}$ of the sensor in (c) the low strain range from 20 to 130% and (d) the high strain range from 130 to 500%. Adapted with permission from ref. 99. Copyright 2020, Royal Society of Chemistry.

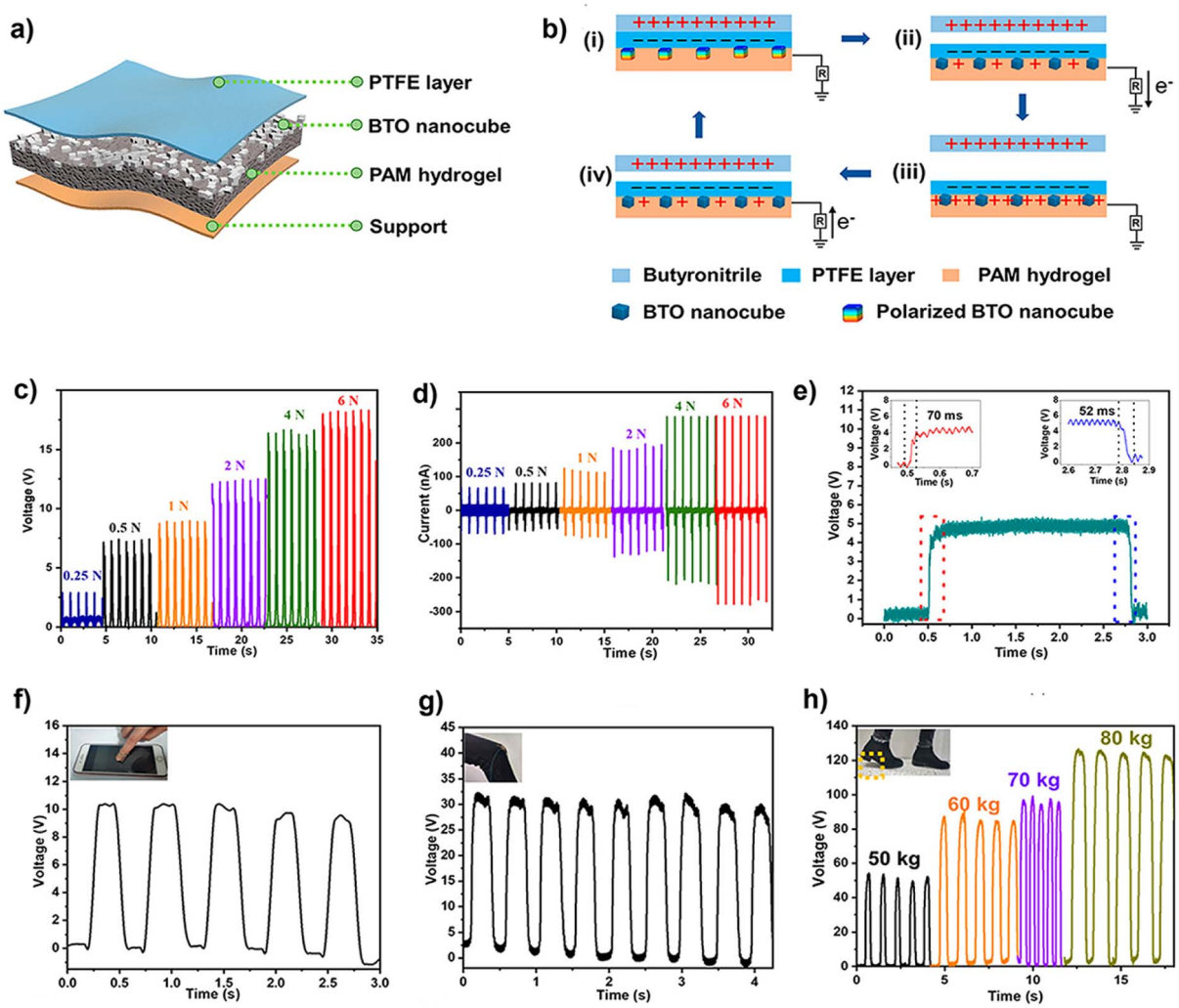

Fig. 8 Performance of the piezoelectric hydrogel strain sensor. (a) Sandwich-like single-electrode piezoelectric barium titanate (BTO) composite hydrogel. (b) Working principle of the hydrogel as a piezoelectric strain sensor. (c) Force-dependent outputs of a BTO composite hydrogel, including open-circuit voltage and (d) short-circuit current and (e) the voltage change of the BTO composite hydrogel as a sensor. Voltage output of the piezoelectric hydrogel sensor attached to different body parts, used for detecting finger pressure on (f) a mobile phone, (g) knee motion, and (h) distinguishing different weights of volunteer students through heel pressure. Adapted with permission from ref. 76. Copyright 2022, American Chemical Society.

Functional properties of hydrogels used in strain sensors

The important functional properties of the hydrogels used in strain sensors are summarized in Fig. 10. To satisfy the requirements for human motion and safe contact with the skin, certain properties such as stretchability, modulus and toughness, recoverability, adhesion, biodegradability, and biocompatibility are primarily required for hydrogel strain sensors.[108,109] Furthermore, antibacterial properties, freeze tolerance, dehydration resistance, and healing properties enhance the adaptability of hydrogel strain sensors from human motion monitoring to other application areas, including soft robotics and human–computer interactions.[110–113] Although previous studies have presented extensive analyses of the functional properties of hydrogels, improvements in one property may negatively affect another. To improve the practical adaptability of strain sensors based on hydrogels, it would be beneficial for a single hydrogel to have multiple properties.

Robust mechanical properties

Mechanical properties, including mechanical strength, toughness, stretching, self-recovery, and fatigue resistance, are essential for hydrogels because they affect the durability and lifetime of hydrogel-based strain sensors. Stronger hydrogels are more resistant to mechanical damage, which improves their overall performance and longevity.[114–117]

Self-healing ability and reusability

Self-healing is a property that allows hydrogels to repair themselves after damage. This feature can be beneficial for strain sensors and wearable devices because it can extend their lifespan.[118,119] In addition, reversible interactions in hydrogels

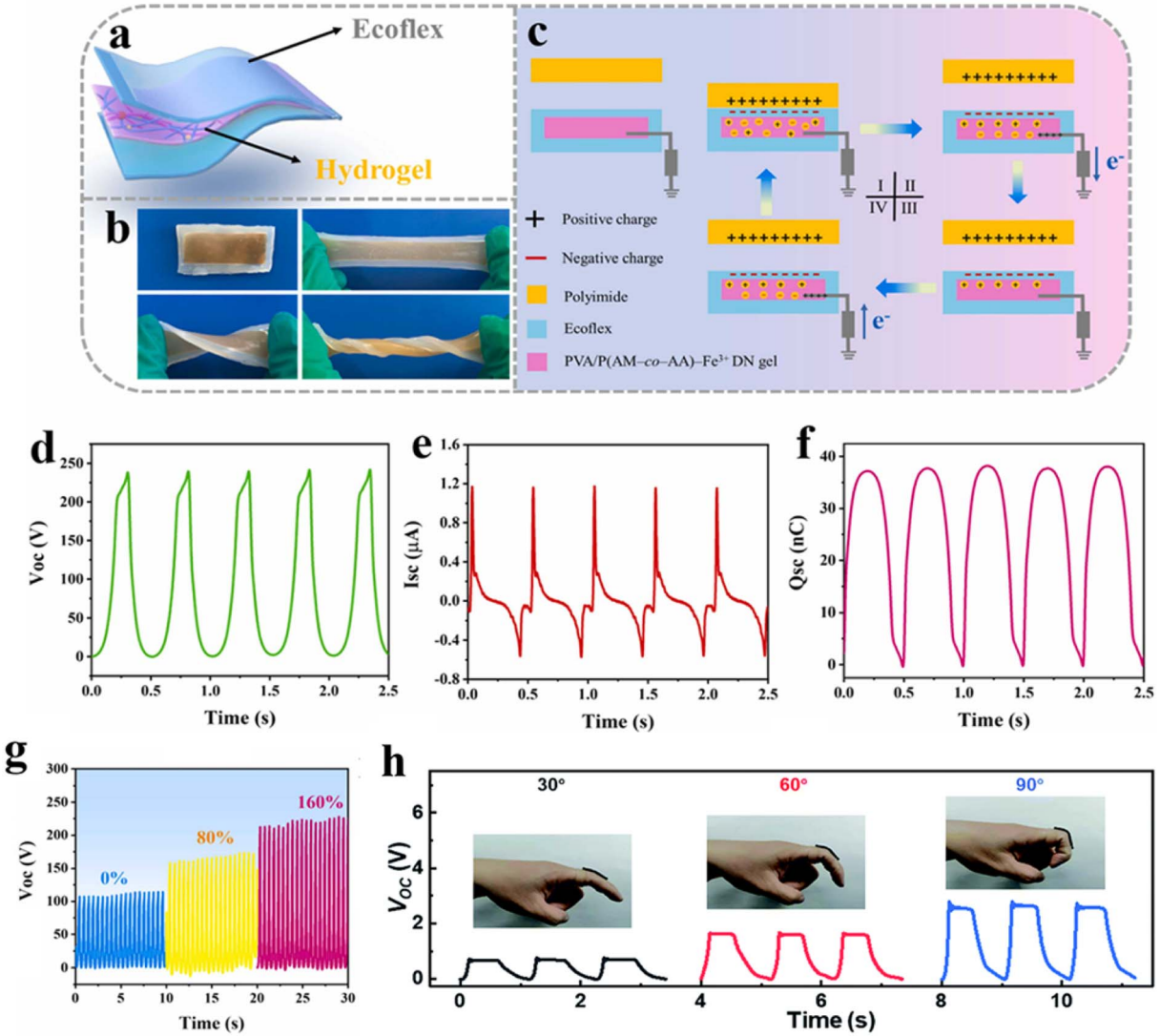

Fig. 9 Performance of the triboelectric hydrogel strain sensor. (a) The structure of a triboelectric generator device, along with digital photos of the sensor in its original, stretched, warped, and twisted states (b). The schematic diagram illustrates the power generation mechanism of the sensor (c). The V_{oc}, I_{sc}, and Q_{sc} of the triboelectric device are plotted in (d), (e), and (f), respectively. (g) The open-circuit voltage of the stretchable triboelectric generator under different strains. Adapted with permission from ref. 105. Copyright 2022, Elsevier. (h) A triboelectric generator device capable of human motion monitoring (adapted from ref. 104). Copyright 2021, Royal Society of Chemistry.

upon heating can provide reusability through reshaping or recycling of hydrogel-based strain sensors to minimize the wastage of hydrogel electronics.[120,121]

Adhesion

Adhesion is important in hydrogels because it affects their ability to function effectively as wearable strain sensors in their intended application. For instance, the hydrogel should adhere consistently and conform to the skin or device surface in human motion monitoring to effectively transfer motion signals.[63,122]

Freezing tolerance and dehydration resistance

The ability of hydrogels to resist freezing at low temperatures, also known as their anti-freezing properties, is an essential property. It is vital in hydrogel-based strain sensors because it retains its sensing performance and functionality in cold environments. Simultaneously, anti-dehydration is the ability of a hydrogel to resist the loss of moisture or water for long-term performance. This is crucial in hydrogel-based strain sensors because they can maintain sensing stability and performance in low-humidity environments.[123,124]

Ultraviolet (UV) radiation blocking properties

Blocking UV radiation can enhance the performance and lifespan of hydrogel-based strain sensors, playing a vital role in protecting hydrogels against discoloration or fading. When used as a wearable strain sensor, it can safeguard skin from UV radiation.[56,125]

Flame retardancy

Flame retardancy in hydrogel-based strain sensors is crucial for resisting ignition and preventing fire spread, especially if

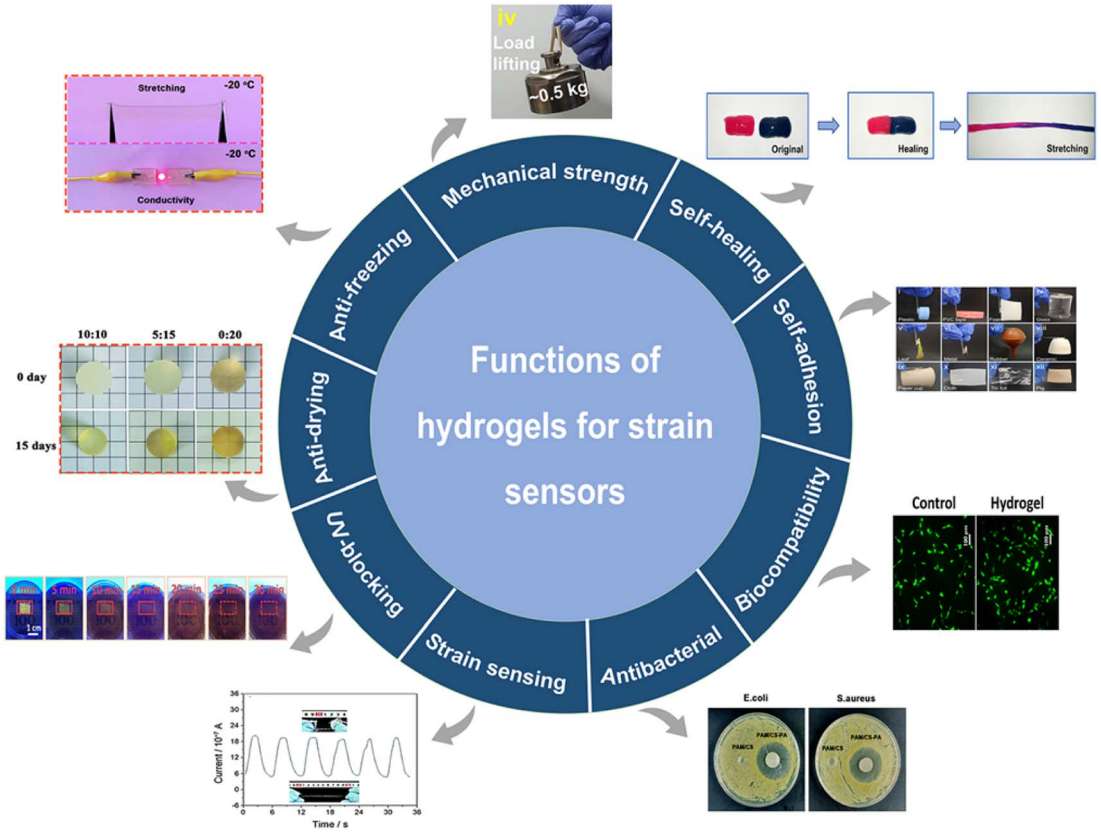

Fig. 10 Important functional properties of hydrogels for strain sensors.

hydrogel-based strain sensors are used in devices or systems prone to overheating.[126,127]

Antibacterial properties

Antibacterial activity is vital for enhancing the safety and performance of hydrogel-based strain sensors in medical applications. It reduces the risk of hydrogel damage due to bacterial growth, improves durability and lifespan, and is a potent solution for wearable hydrogel-based strain sensors.[93,128]

Biocompatibility

Biocompatibility is crucial for developing hydrogel-based strain sensors, which are often used in wearable or implantable biomedical applications and encounter living tissues. For example, hydrogel-based strain sensors have been used on the skin for human motion detection. Therefore, hydrogels should be skin-friendly and not cause adverse effects, such as toxicity or allergic reactions, affecting the tissue or an individual's overall health.[129–131]

Strain sensing

Although electrical conductivity is not essential in all strain-sensing mechanisms, it is necessary in piezoresistive hydrogel-based strain sensors because it allows the detection of changes in strain by measuring the changes in electrical resistance. When a hydrogel is stretched or compressed, its electrical resistance changes, which can be measured and used to determine the amount of strain.[47,132,133]

Status of performance indicators of strain sensors based on hydrogels

Hydrogel-based strain sensors have made significant progress in recent years in terms of their performance indicators, such as a wide working range, linearity of the working range, sensitivity, response/recovery time, and hysteresis.

Wide working range

The working range indicates the maximum and minimum strain values that could be accurately measured using a hydrogel-based strain sensor. This range is closely related to the type of application in which the strain sensors are used. For example, a strain sensor with a broad working range can detect signals when a large strain value is involved. However, a small working range is sufficient to detect small strain values. Moreover, the wide working range makes hydrogel-based strain sensors versatile, facilitating their usage in various applications, including wearable devices, soft robotics, biomedical engineering, and human–machine interfaces. The working range directly relates to safe stretchable limits without any fracture or discrepancy in the hydrogel, which could negatively affect the structure of the hydrogel and its strain-sensing ability.

Linearity of the working range

The linear working range of the hydrogel-based strain sensor indicates that the sensor exhibits uniform strain sensing across its entire working range. This enables more accurate and precise strain measurements, simplicity in interpreting and processing the data, and easier calibration of hydrogel-based strain sensors.

Sensitivity

Sensitivity refers to the ability of a hydrogel-based strain sensor to detect and convert strain signals into electrical signals within a suitable working range. Highly sensitive sensors can efficiently capture even minor fluctuations in strain.

Response/recovery time

The response time of a hydrogel-based strain sensor is a measure of how quickly it responds to strain changes. A shorter response time implies that the sensor can perform real-time monitoring tasks and precisely track dynamic variations in strain. In contrast, the recovery time of a hydrogel-based strain sensor is the interval between the removal of the external deformation and the return of the sensor to its initial or baseline state. This characteristic reflects the capability of the sensor to recover from the deformation and prepare for further measurements promptly. The shorter recovery period indicated that the sensor could promptly revert to its initial state, enabling it to perform multiple strain measurements shortly with maximum efficiency.

Hysteresis

In hydrogel-based strain sensors, hysteresis refers to the inability of the sensor output to revert to its initial state, causing irregularities in the response. This inconsistency in real-time sensing data acquisition can lead to inaccurate strain monitoring. A low hysteresis is preferable for an excellent strain sensor, resulting in accuracy, consistency, repeatability, and a linear range of strain sensing.

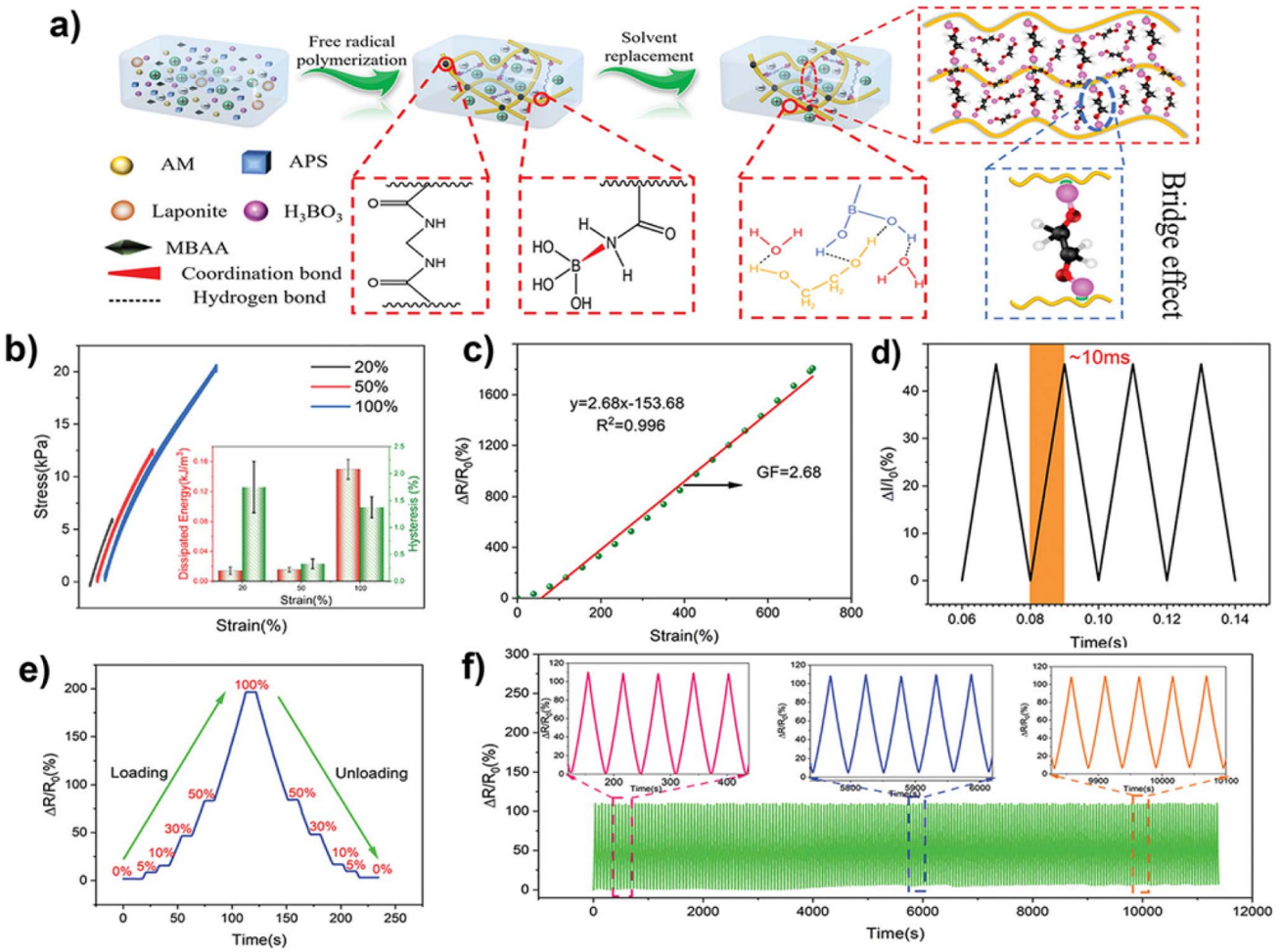

Fig. 11 Performance indicators of strain sensors based on hydrogels. (a) A diagrammatic representation of the fabrication process for PLBOH and its internal interactions. (b) Various strains applied for 10 cycles (the inset displays the energy dissipation and hysteresis). (c) The change in relative resistance across a wide strain range of 0–750% with the linearity of the working range and the associated GF (sensitivity) for the strain sensor. (d) The response time of the strain sensor when the wrist is bent quickly. (e) The $\Delta R/R_0$ of the gel when subjected to stepwise strain (0–100%) in its as-prepared state. (f) The $\Delta R/R_0$ of the strain sensor when subjected to 100% strain for 200 cycles without any resting time, at a speed of 20 mm per minute. Adapted with permission from ref. 134. Copyright 2023, John Wiley and Sons.

According to the latest research trends, an optimal hydrogel-based strain sensor should display all these performance indicators at the best possible level.[134–136] Zhou *et al.* presented a strain sensor composed of a polyacrylamide (PAM)/LAPONITE®/boric acid/ethylene glycol (E_g) organohydrogel (PLBOH), as shown in Fig. 11. This sensor demonstrated exceptionally low hysteresis (1.38% at a tensile strain of 100%), ultrafast response time (approximately 10 ms), and high linearity throughout a wide strain range ($R^2 = 0.996$), along with sensitivity (GF of 2.68 in the 0–750% strain range).

The minimal hysteresis was ascribed to the rapid disintegration and reformation of the hydrogen (H) and B^{3+} complex coordination bonds. This process guaranteed that the internal structure remained synchronized with the external deformation on an equivalent timescale. This is in accordance with the relaxation rate and supports the high-linearity working range of strain sensing, which further supports the high strain sensitivity, fast response/recovery, stability, and repeatable strain-sensing attributes.

Small biomolecules for hydrogel-based strain sensors

Citric acid (CA)

Citric acid (chemical formula: $C_6H_8O_7 \cdot H_2O$, molecular weight: 192.1 g mol^{-1}) is a tricarboxylic acid and a natural compound that can be produced biologically by the fermentation of plant biomass, citrus fruits, and pineapples.[137–139] The industrial-scale production of CA from biological sources by chemical methods involves several steps. In a typical procedure, orange, grape, lemon, or pineapple juices are first neutralized to pH 10 using an alkali solution such as calcium oxide, calcium carbonate, or

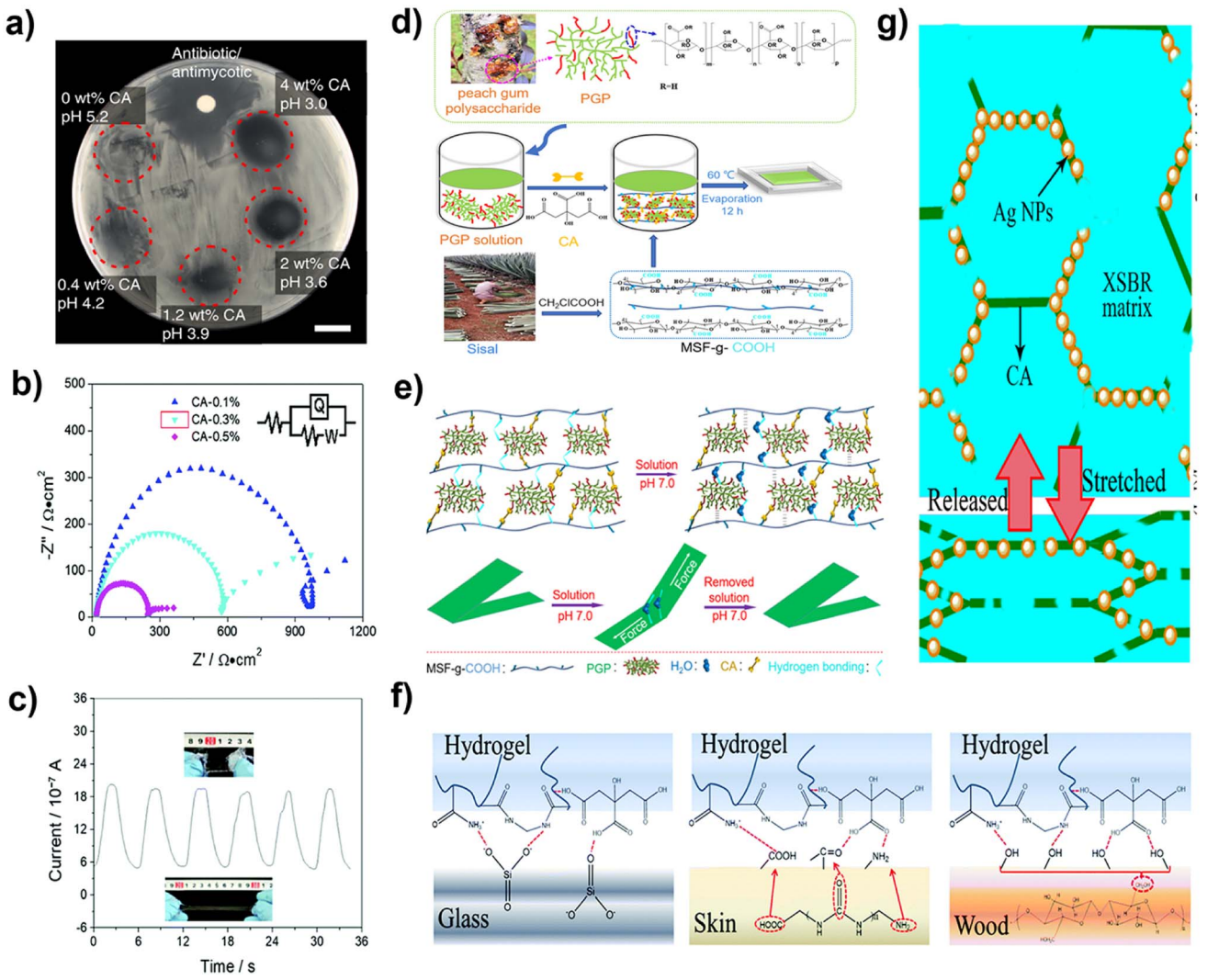

Fig. 12 (a) Antibacterial properties of hydrogel strain sensors at various concentrations of CA.[151] Copyright 2020, Springer Nature BV. (b) EIS curves depicting ionic conductivity as a function of CA concentration from 0.1 to 0.5 wt% and (c) its potential as a strain sensor.[152] Copyright 2020, Royal Society of Chemistry. (d) Crosslinking capacity of CA with sisal microcrystals and peach gum polysaccharide polymer chains *via* esterification and (e) shape memory effects.[153] Copyright 2021, Elsevier. (f) CA as a promoter of adhesive properties in hydrogel strain sensors.[152] Copyright 2020, Royal Society of Chemistry. (g) Conduction mechanism of CA-based sensors for human motion monitoring.[154] Adapted with permission from ref. 154. Copyright 2020, American Chemical Society.

sodium hydroxide. Calcium citrate was precipitated using calcium chloride and subsequently acidified with dilute sulfuric acid to yield calcium sulfate and crystallized CA.[140] CA is also a byproduct of various biological and chemical reactions.[141–143] More recently, CA has been produced by microbes, such as the filamentous fungus Aspergillus niger. In a typical study, Aspergillus niger was isolated from spoiled coconuts at pH 3.5 and 30 °C, producing approximately 80 g L^{-1} of CA.[144]

The conjugation of functionalized NPs with CA showed cytocompatibility, having a cell viability above 110% for MCF7 cells after 24 h and for MC3T3-E1 cells.[145,146] The copolymerization and modification of CA with other synthetic monomers have also demonstrated biodegradability and biocompatibility.[147,148] These studies indicated that using CA in hydrogel strain sensors is biologically safe.

CA has been reported to have antibacterial and cross-linking effects in hydrogels;[149,150] thus, the same is expected in hydrogel strain sensors. For example, Baumgartner *et al.* developed a degradable gelatin-based gel for measuring strain, pressure, and other sensors using CA.[151] Increasing the CA concentration to 4 wt% improved the antibacterial properties in the diffusion disc test, resulting in an enlargement of the bacterial inhibition zone, as shown in Fig. 12(a).

Z. Li *et al.* demonstrated that CA endows a hydrogel with improved ionic conductivity, as indicated by a reduction in the semicircle size in the electrochemical impedance spectroscopy (EIS) curves (Fig. 12(b)) for human motion monitoring (Fig. 12(c)).[152] Furthermore, CA endows hydrogels with a shape-memory effect. For instance, Zhang *et al.* reported that CA cross-linked sisal cellulose microcrystals and peach gum polysaccharide molecules through an esterification reaction in smart films, as shown in Fig. 12(d).[153] Cross-linking with CA provided a moisture-induced shape-memory effect owing to changes in the polymer network under different pH conditions (Fig. 12(e)). Although CA has demonstrated various properties of conductive hydrogels, little attention has been paid to fine-tuning their mechanical properties. In fact, mechanical toughness has been reported to decrease with increasing CA concentration.[151]

Furthermore, at a CA concentration of 0.1%, CA molecular interactions can impart adhesive properties to hydrogels for various substrates such as glass, skin, and wood, as shown in Fig. 12(f). Chuanhui *et al.* reported that CA could reduce the Ag ions (Ag^+) produced from the ionization of AgCl salt in strain sensor systems to introduce various functions such as electrical conductivity and antibacterial effects.[154,155] Ultimately, the AgNPs imparted conductive properties to the hydrogel for piezoresistive strain sensing when stretched and released, as shown in Fig. 12(g). Fruit-derived malic acid has similar functions in hydrogels for strain sensors.[156]

Zwitterionic osmolytes

Zwitterionic osmolytes, such as betaine (molecular weight: 117.1 g mol^{-1}) and proline (molecular weight: 115.1 g mol^{-1}), are naturally derived compounds that play a crucial role in regulating the balance of water and solutes in living organisms.[157] For instance, betaine can be extracted from beet molasses using the cloud-point extraction technique, which is a fast, simple, and environmentally friendly process with yields of up to 80%.[158] Betaine can also be isolated from various *B. vulgaris* varieties using accelerated solvent extraction combined with solid-phase extraction with up to 90% efficiency.[159] Proline is a water-soluble amino acid containing an α-imino group and possesses a unique ring structure. It is abundant in collagen-rich compounds, such as cheese, soybeans, and collagen. However, milk, eggs, seeds, and legumes contain low levels of proline. Proline also accumulates in plants in response to stress.[160–162] These molecules are called "zwitterionic" because they have both positive and negative charges in the same molecule.

Betaine and proline are both biocompatible molecules. In a clinical study, betaine exhibited 85% cell viability after two days in an assay of live/dead cell chondrocytes, NIH-3T3 fibroblasts, and human umbilical vein endothelial cells (HUVECs) with a normal spindle-like morphology.[163,164] High resistance to nonspecific protein absorption supports biocompatibility owing to the high hydrophilicity of the betaine moieties.[165] Similarly, proline exhibited biocompatibility and antifouling properties in hydrogel strain sensors. For example, a hydrogel strain sensor composed of gellan gum (GG) and PAM exhibited more than 80% cell viability after two days in the CCK-8 assay, as shown in Fig. 13(a). In addition, the proline-containing hydrogel strain sensor showed a 94.4% decrease in protein absorption compared with the control sample, suggesting excellent antifouling properties, as shown in Fig. 13(b).[57] Xinyu *et al.* reported a hydrogel strain sensor for tissue-attached sensing applications using proline[166] (Fig. 13(c)).

Furthermore, the betaine and proline molecules interact perfectly with water molecules, making them resistant to ice formation at subzero temperatures. This property of freezing tolerance performs useful biological functions in plants, such as reducing fruit damage from the cold and providing plants with osmotic protection to endure abiotic stress for survival.[167–170] In particular, barley increases the production of these molecules during winter to provide freezing tolerance and to withstand environmental stress.[171]

Inspired by their freeze-tolerance effect on water, researchers have used betaine[172–174] and proline[57,175–177] to achieve freeze tolerance in hydrogel strain sensors and maintain their functions at sub-zero temperatures. For instance, Jiao *et al.* developed a hydrogel composed of GG/PAM/proline strain sensor, which successfully preserved the electrochemical functions at −40 °C, demonstrating the interaction of the $-NH_2^+$ and $-COO^-$ groups of proline with water to provide freeze tolerance, as shown in Fig. 13(d).[57] Similarly, Feng *et al.* reported that betaine improved the freeze tolerance of hydrogel strain sensors composed of a polyacrylic acid (PAA)-Al^{3+}/poly(3,4-ethylenedioxythiophene) polystyrene sulfonate (PEDOT:PSS) network, allowing the hydrogel strain sensors to remain flexible under harsh climatic conditions of −35 °C.[178]

Moreover, the ionic sites on proline enhance its mechanical properties and adhesion to the skin.[57,179] Mechanical properties such as stretchability (~1800%), elastic moduli, and toughness

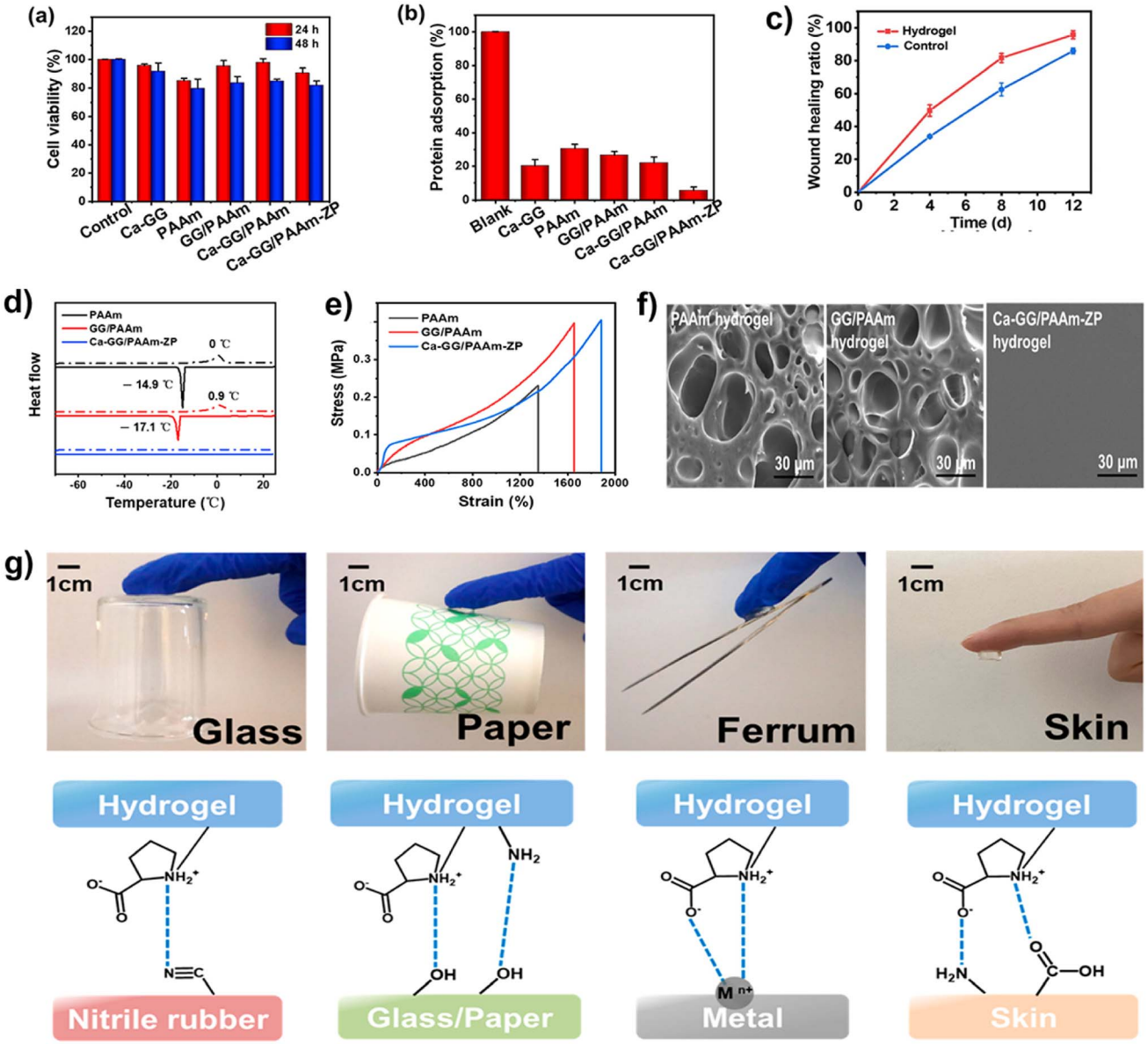

Fig. 13 (a) The role of zwitterionic proline (ZP) in the cell viability of the gellan gum (GG)/PAM hydrogel strain sensor for biocompatibility and (b) the effect of ZP on protein adsorption in the GG/PAM hydrogel strain sensor for antifouling properties.[57] Adapted with permission from ref. 57. Copyright 2021, American Chemical Society. (c) ZP improves the wound healing rate in mice using the proposed bilayer hydrogel for strain sensor.[166] Copyright 2021, Elsevier. (d) Differential scanning calorimetry curves of the GG/PAM hydrogel strain sensor demonstrating freezing tolerance behavior, (e) the effect of ZP on the tensile stress–strain behavior of the hydrogel strain sensor, (f) densification of the microporous structure in GG/PAM hydrogels in the presence of ZP, and (g) illustration of the role of ZP for the adhesion characteristics between the GG/PAM hydrogel and various substrates.[57] Adapted with permission from ref. 57. Copyright 2021 American Chemical Society.

are improved owing to the $-NH_2^+$ site of proline, which forms H bonds with the $-COO^-$ groups of GG polymer chains (Fig. 13(e)), which densifies into a microporous structure of the hydrogels studied under scanning electron microscopy (Fig. 13(f)). Furthermore, zwitterionic molecules impart adhesion properties to hydrogels for attachment to various substrates (Fig. 13(g)).

Tannic acid (TA)

TA, a natural polyphenol with a high molecular weight of 1701.19 g mol^{-1}, is a water-soluble amphiphilic compound commonly found in plants, red wine, grapes, and tea extracts. The general chemical structure of TA is ($C_{76}H_{52}O_{46}$) with multiple pyrogallol and catechol groups.[31,180,181] It contains many –OH and –COOH groups that confer polyacid properties.[182,183] Tannin extraction is performed using several methods, such as the following extractions: solid–liquid, supercritical fluid, pressurized water, microwave-assisted, supercritical fluid, and ultrasound-assisted.[184,185]

As a cross-linking molecule, TA can form H bonds with functional groups on other polymers such as silk, gelatin, CS, and PVA to enhance the mechanical properties of conductive

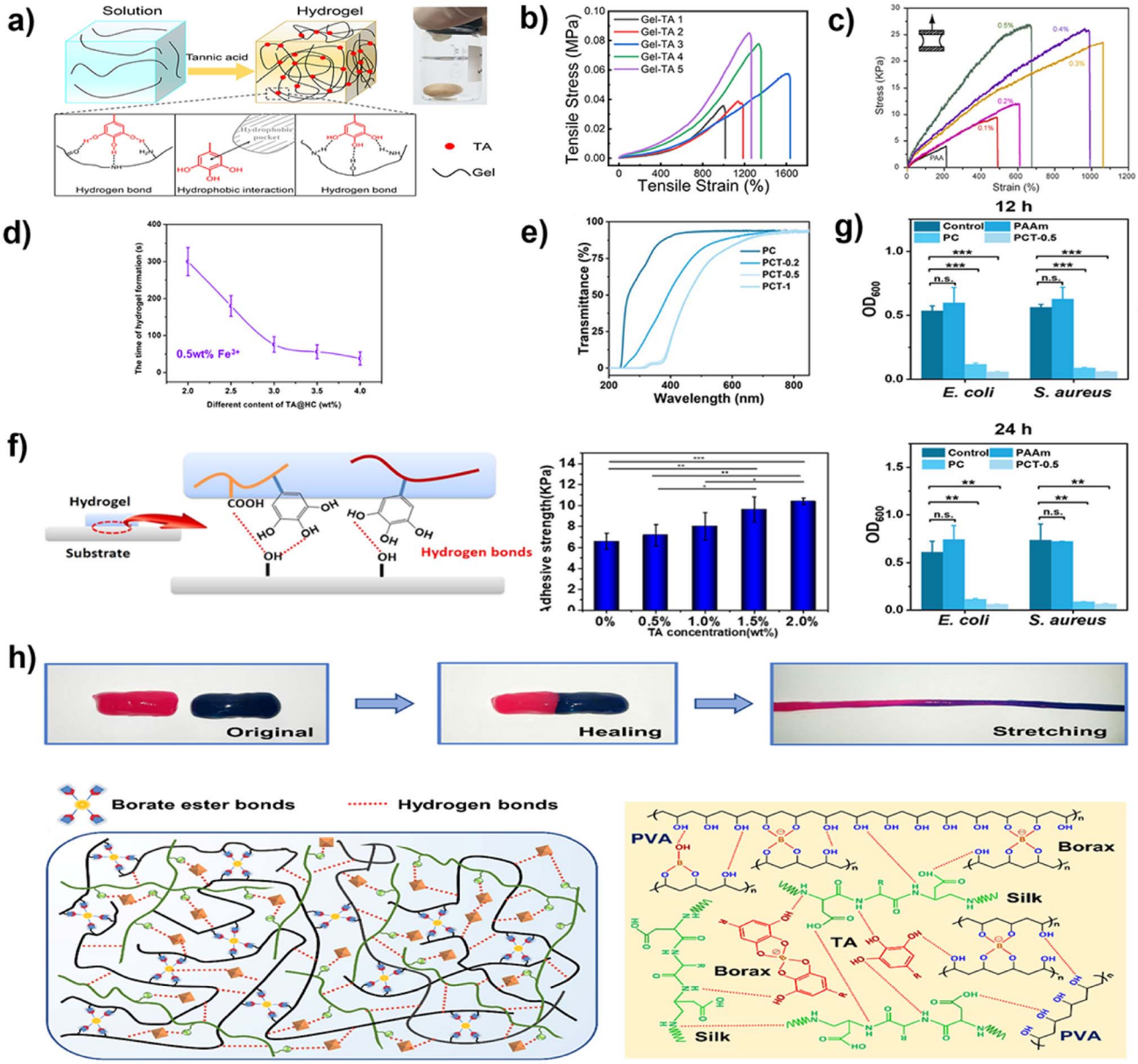

Fig. 14 (a) The role of TA in hydrogen (H) bonding and hydrophobic interactions with gelatin (Gel) polymer chains in platforms for hydrogel strain sensors and (b) tensile stress–strain behavior of Gel-TA hydrogels at various TA concentrations for strain sensors.[52] Adapted with permission from ref. 52. Copyright 2020, American Chemical Society. (c) TA-coated hemicellulose improves mechanical properties in PAA/TA@hemicellulose/Al^{3+} hydrogels as a function of TA content for strain sensors.[196] Copyright 2021, Elsevier. (d) Effect of TA on the radical polymerization rate for enhanced gelation rates forming conductive PAA/TA@hemicellulose/Fe^{3+} hydrogels for strain sensors.[197] Adapted with permission from ref. 197. Copyright 2022, American Chemical Society. (e) Effect of TA concentration on the UV-blocking properties in PAM/CS/TA (PCT) hydrogel strain sensors.[55] Copyright 2021, John Wiley and Sons. (f) Mechanism of adhesive properties in hydrogel strain sensors as a function of TA.[123] Adapted with permission from ref. 123. Copyright 2021, American Chemical Society. (g) Antibacterial activity as a function of TA in PCT hydrogel strain sensors.[55] Copyright 2021, John Wiley and Sons. (h) Reversible non-covalent interactions in the presence of TA for self-healing characteristics in hydrogel strain sensors.[186] Adapted with permission from ref. 186. Copyright 2021 American Chemical Society.

hydrogels for strain sensors.[186–192] The –OH groups and benzene rings in the polyphenolic moieties can cross-link the gelatin polymer chains through H bonds and hydrophobic interactions (Fig. 14(a)), thereby improving the mechanical properties with increasing TA content in the hydrogel (Fig. 14(b)). The proposed hydrogel exhibited an excellent stretchability of 1600% as a platform for fabricating strain sensors incorporating conductive nanomaterials.[52] TA has also been used to coat nanomaterials to improve the mechanical properties of hydrogel strain sensors.[193–195]

Gong *et al.* coated hemicellulose NPs with TA and applied them to a polyacrylic-acid-based hydrogel. The catechol groups on the TA-modified hemicellulose NPs enhanced mechanical properties such as tensile strength, which increased from 7.5 to

27.5 kPa (Fig. 14(c)). They provided dynamic linking bridges through the aluminum cation (Al^{3+}) with PAA chains or among TA-modified NPs, resulting in high compression strength, stretchability up to 1060%, toughness up to 1.52 MJ m^{-3}, and self-recovery with an efficiency of 87%.[196] An extended study using Fe^{3+} and Ag^{+} ions instead of Al^{3+} has been reported,[197,198] which showed a rapid gelation process in acrylic acid monomers to form PAA/TA@hemicellulose/Fe^{3+} hydrogels, as shown in Fig. 14(d). Furthermore, TA-Fe^{3+} complexes provide hydrogel strain sensors with excellent adhesion to the skin for use as wearable strain sensors.[199] Comparable studies have reported similar findings for hydrogel strain sensors using TA-coated cellulose nanofibers/cellulose nanocrystals, graphene oxide, carbon nanotubes, and talc.[200–204]

Furthermore, TA imparts UV-blocking, adhesion, and antibacterial properties to hydrogel strain sensors because of its polyphenolic groups.[55,56,123,205] Sun *et al.* fabricated a hydrogel strain sensor from a PAM/CS/TA hydrogel. The hydrogel exhibited over 96% UV blocking by absorbing UV radiation in the 350–390 nm range (Fig. 14(e)).[55,206] Additionally, the hydrogel showed over 97% antibacterial activity against *E. coli* and *S. aureus* bacteria, as measured from optical density (OD) after 12 and 24 h (Fig. 14(g)).[55] The catechol properties of TA make hydrogel adhesives useful for hydrogel strain sensor applications on the skin, and the adhesion increases with increasing TA content (wt%) (Fig. 14(f)).[122,123]

TA can endow hydrogel-based strain sensors with the self-healing properties of hydrogels composed of protein polymer chains such as silk, gelatin, and copolymerized synthetic networks.[110,186–188] For example, Zheng *et al.* reported that the polyphenolic catechol groups on TA molecules improved their self-healing properties by forming dynamic H bonds to reconnect the broken bonds of –COOH and $–NH_2$ groups on silk fibroin polymer chains, –OH groups on PVA, and coordination with borate ions. The resultant hydrogels exhibited excellent stretchability (above 1000%) and self-healing efficiency (above 85%) within 30 s without any external stimulus (Fig. 14(h)).[186] A similar self-healing mechanism through TA-coated cellulose nanocrystals can form dynamic H bonds with PAA polymer chains in a chemically cross-linked network.[207]

TA ensures biocompatibility in hydrogel strain sensors because it is naturally derived from plants and is of biological origin.[200,208] Zheng *et al.* reported that TA in conductive hydrogels composed of PVA, borax, and silk fibroin (PBST hydrogel) exhibited biocompatibility. Biocompatibility was evaluated by a cytotoxicity test (CCK-8 analysis) using mouse fibroblast cells and by observing the cell morphology using a confocal laser microscope. The results showed that the cells adhered well to the surface of the hydrogel (Fig. 15(b)) and grew, showing cell proliferation during the 7 d of culture (Fig. 15(a)). Cell proliferation and adhesion were observed with increasing concentrations of TA, suggesting good biocompatibility.[186,187] In another study, the TA-based PAM/CS hydrogel was biocompatible, exhibiting over 100% viability of L920 cells in the CCK-8 assay (Fig. 15(c)). The cells exhibited a high-density spindle-like morphology.[55] However, the concentration of TA in the hydrogel strain sensors should be carefully optimized; otherwise, cytotoxicity may occur at much higher concentrations. For example, Zhao *et al.* reported the minor cytotoxic effects of PVA/sodium alginate/borax hydrogels and PAM/sodium alginate hydrogels for strain sensors, exhibiting a cell viability of over 80% after 72 h.[42,209]

TA has been reported to modify the electrical conductivity and strain sensitivity of hydrogel strain sensors. Zaidi *et al.*

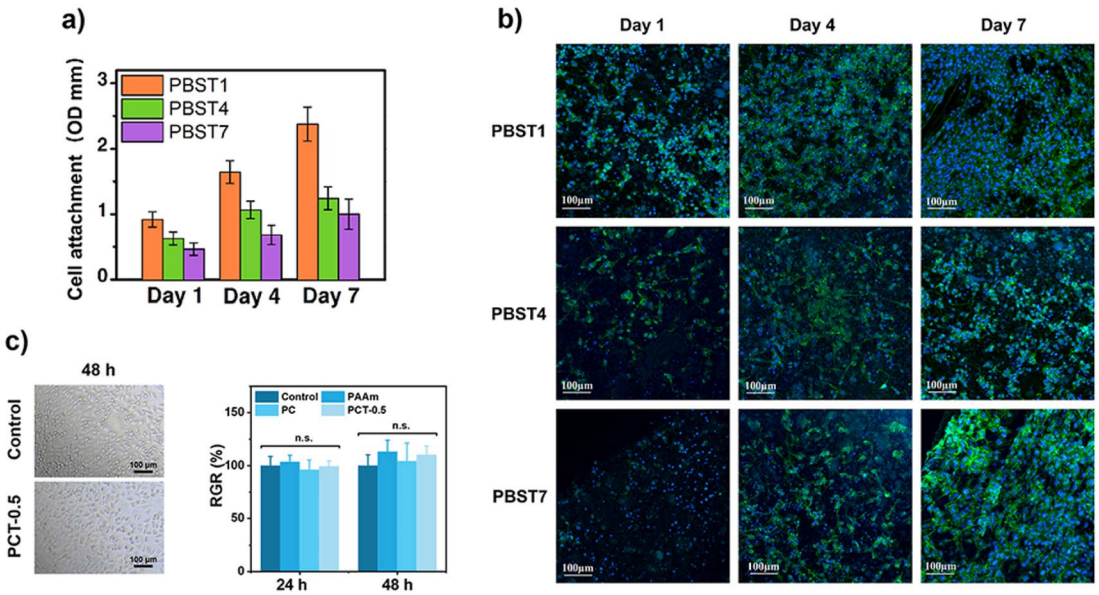

Fig. 15 (a) CCK8-cell proliferation assay of PVA/borax/silk fibroin/TA (PBST) hydrogels for strain sensors at various concentrations of TA and (b) confocal laser microscope images of mouse fibroblasts on the surface of the PBST-4 hydrogel for 1, 4, and 7 days.[186] Adapted with permission from ref. 186. Copyright 2021 American Chemical Society. (c) Biocompatibility results of PAM/CS/TA hydrogel strain sensors (RGR = relative growth rate).[55] Copyright 2021, John Wiley and Sons.

proposed a TA-modified ion-conducting gelatin organohydrogel using sodium citrate and sodium chloride salts (GEL/$Gel_{(30)}$/TA), as shown in Fig. 16(a). The modification provided a unique, interconnected hierarchical porous structure of the gels that exhibited a simultaneous increase in pore size and pore wall thickness, resulting in low modulus and high toughness values, considering the wearability of the strain sensors. Moreover, the microstructural details of the gels suggested an improvement in ionic conductivity (up to 0.8 S m^{-1}) and tunability of strain sensitivity (maximum up to GF = 6.5). The proposed organohydrogel showed the potential to monitor human motion from large to small scales (Fig. 16(b)).[51]

Phytic acid (PA)

PA contains a high phosphorus and carbon content, making it a biogenic and non-toxic compound. PA is naturally derived from oilseeds, legumes, cereals, nuts, fruits, vegetables, pollen, seeds, roots, and plant stems. The molecular formula of PA is $C_6H_{18}O_{24}P_6$ (molecular weight: 660.04 g mol^{-1}), also known as *myo*-inositol (1,2,3,4,5,6) hexakisphosphoric acid.[210–212] It is considered a poly-acid because it contains six phosphate groups that can ionize in aqueous solutions and release multiple H ions (H^+).[213,214]

PA extraction includes PA solubilization and acid dissociation. Various methods of PA extraction have been explored using

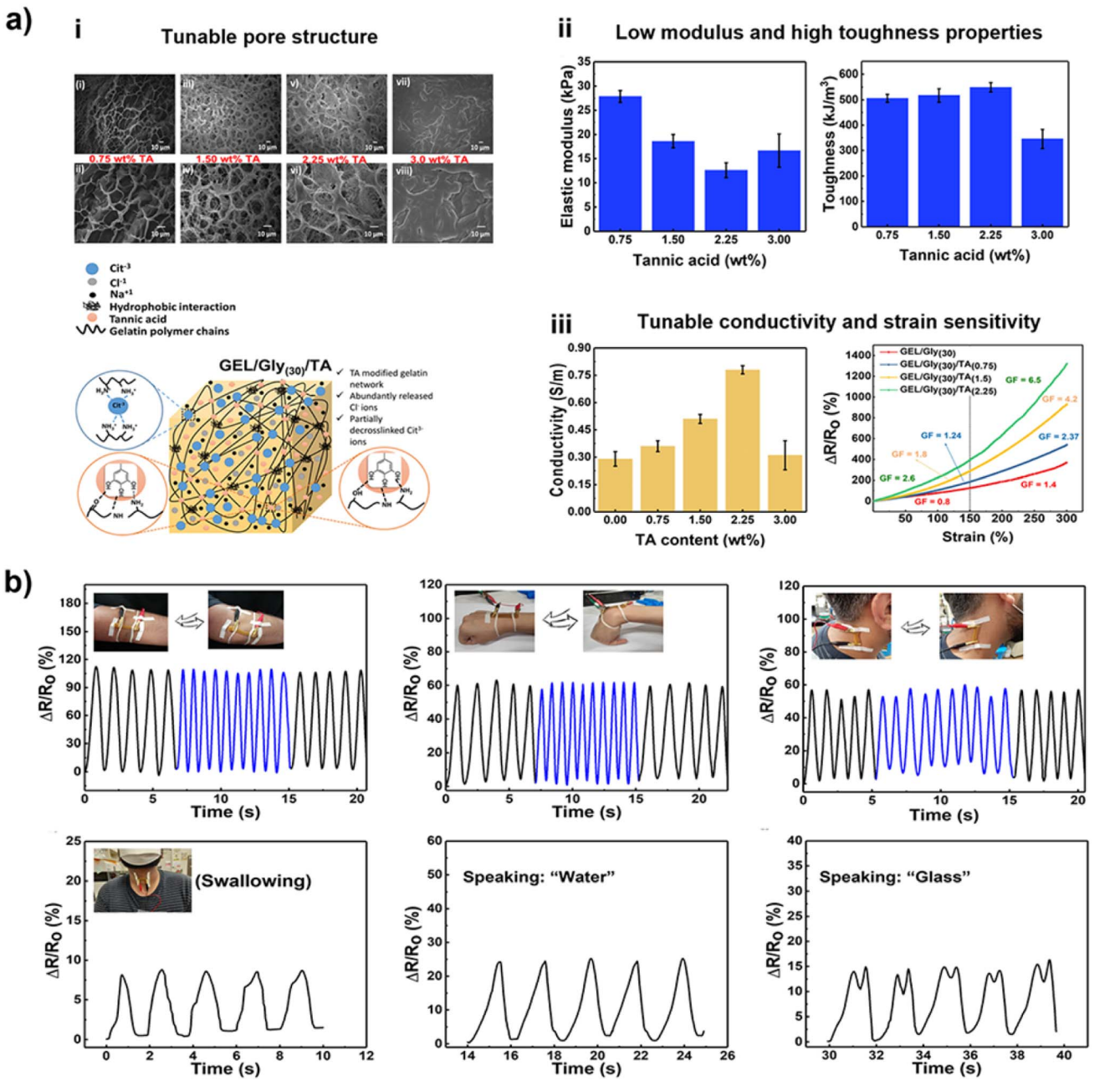

Fig. 16 GEL/$Gly_{(30)}$/TA organohydrogel as a strain sensor for monitoring human motion (adapted from ref. 51). (a) Scheme of the tunable pore morphology, mechanical properties, ionic conductivity, and strain sensitivity of the organohydrogel. (b) The potential to monitor human motions from large to small scales. Copyright 2022, Elsevier.

different acidic solutions. For example, hydrochloric acid (HCl) extracted 182.7 mg g^{-1} dry PA from peanuts. The response surface methodology was used to optimize the extraction conditions, in which an HCl concentration of 0.02 mol L^{-1}, a solid-to-liquid ratio of 1 : 16 (g : mL), an extraction temperature of 30 °C, and an extraction time of 105 min were optimized.[212,215]

PA acts bifunctionally as a cross-linker and a source of ionic conduction in hydrogel strain sensors.[69,216,217] PA formed H bonds with the polymer chains in the hydrogels that contributed to physical cross-linking, ultimately leading to improved mechanical properties, as shown in Fig. 17(a). Cross-linking improves mechanical properties. For example, the tensile

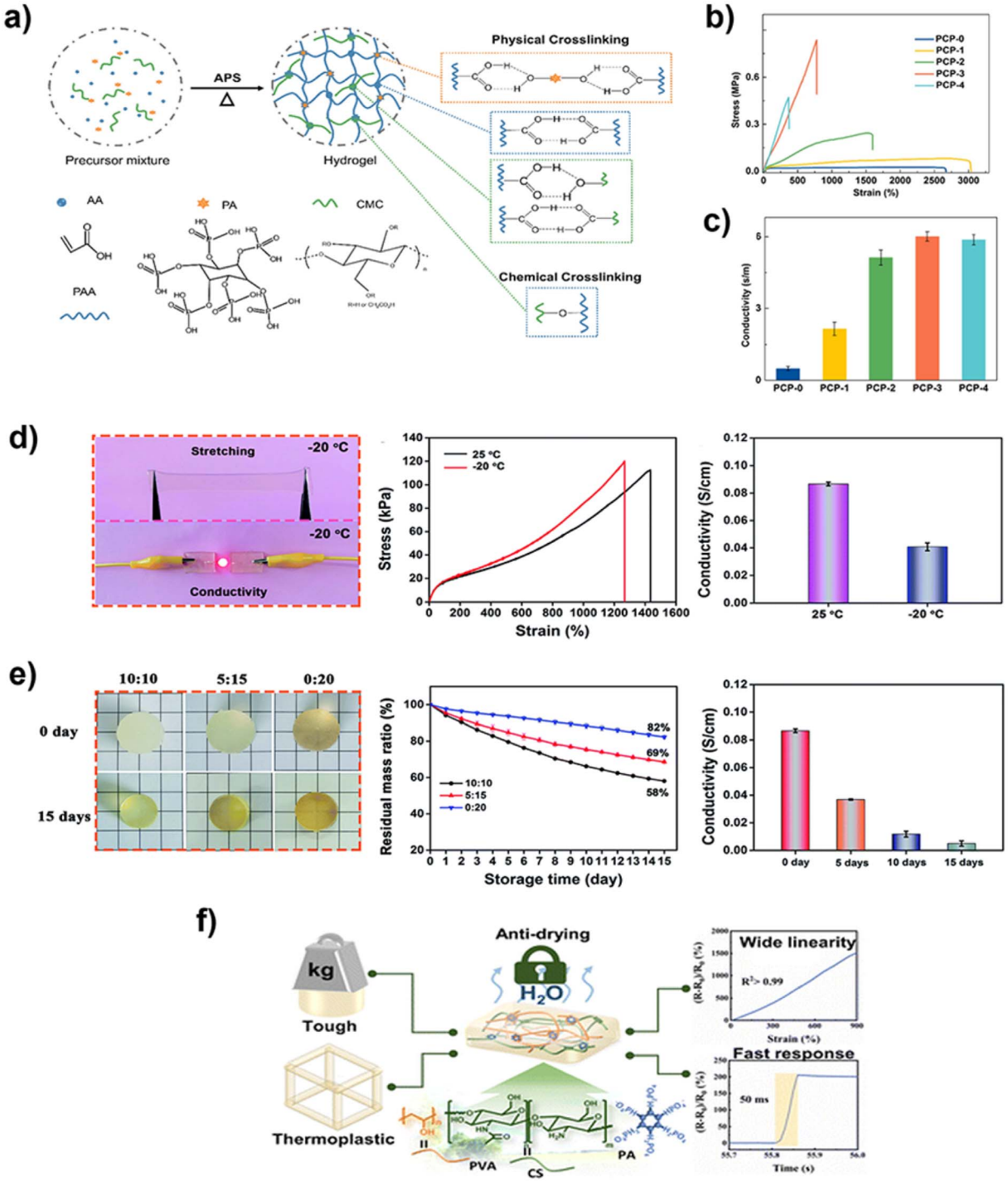

Fig. 17 (a) Cross-linking ability of PA in polyacrylic acid (PAA)/carboxymethyl cellulose (CMC) hydrogels for strain sensors, (b) tensile stress–strain behavior in PAA/CMC/PA (PCP) hydrogels at various concentrations of PA, and (c) ionic conductivity as a function of PA content in PCP hydrogels.[219] Copyright 2021, Springer Nature B.V. (d) PA function for freezing tolerance and (e) dehydration resistance in hydrogels for strain sensors.[44] Copyright 2021, Royal Society of Chemistry. (f) Cross-linking of PVA/CS hydrogels with PA, resulting in toughness, thermoplasticity, anti-drying, wide linear strain sensing range, and fast sensing response.[45] Copyright 2023, Royal Society of Chemistry.

strength increases from 0.07 to ~0.9 MPa (Fig. 17(b)). Simultaneously, PA can provide hydrogels with ionic conductivities up to 6 S m^{-1} (Fig. 17(c)). Furthermore, PA imparts excellent freeze-tolerance and anti-drying properties to hydrogel strain sensors.[44,218] In a report, PA also endowed the hydrogel with excellent freezing tolerance at −20 °C, demonstrating an ionic conductivity of 0.04 S cm^{-1} without loss of mechanical flexibility of the hydrogel. Moreover, PA imparts dehydration resistance to the hydrogels (82% weight retention after 15 days in a 75% relative humidity environment), maintaining a conductivity of 0.01 S cm^{-1} on the 15th day of the dehydration experiment (Fig. 17(e)). Furthermore, Liu *et al.* reported a PA-containing PVA/CS hydrogel strain sensor that showed a wide linear operating range of up to 900% strain, a fast response time of 50 ms, and thermoplastic behavior for reusability combined with improved toughness and ductility, as shown in Fig. 17(f). Additionally, the hydrogel strain sensor retained more than 90% of the water after 30 days due to PA.[45]

PA also imparts antibacterial properties to hydrogel strain sensors. Fig. 18(a) depicts the antibacterial properties of the PA-containing hydrogels against *E. coli* and *S. aureus* bacteria using the diffusion disc test, which exhibited a large zone of bacterial growth inhibition. Furthermore, strong reversible noncovalent interactions with the polar functional groups in the hydrogel

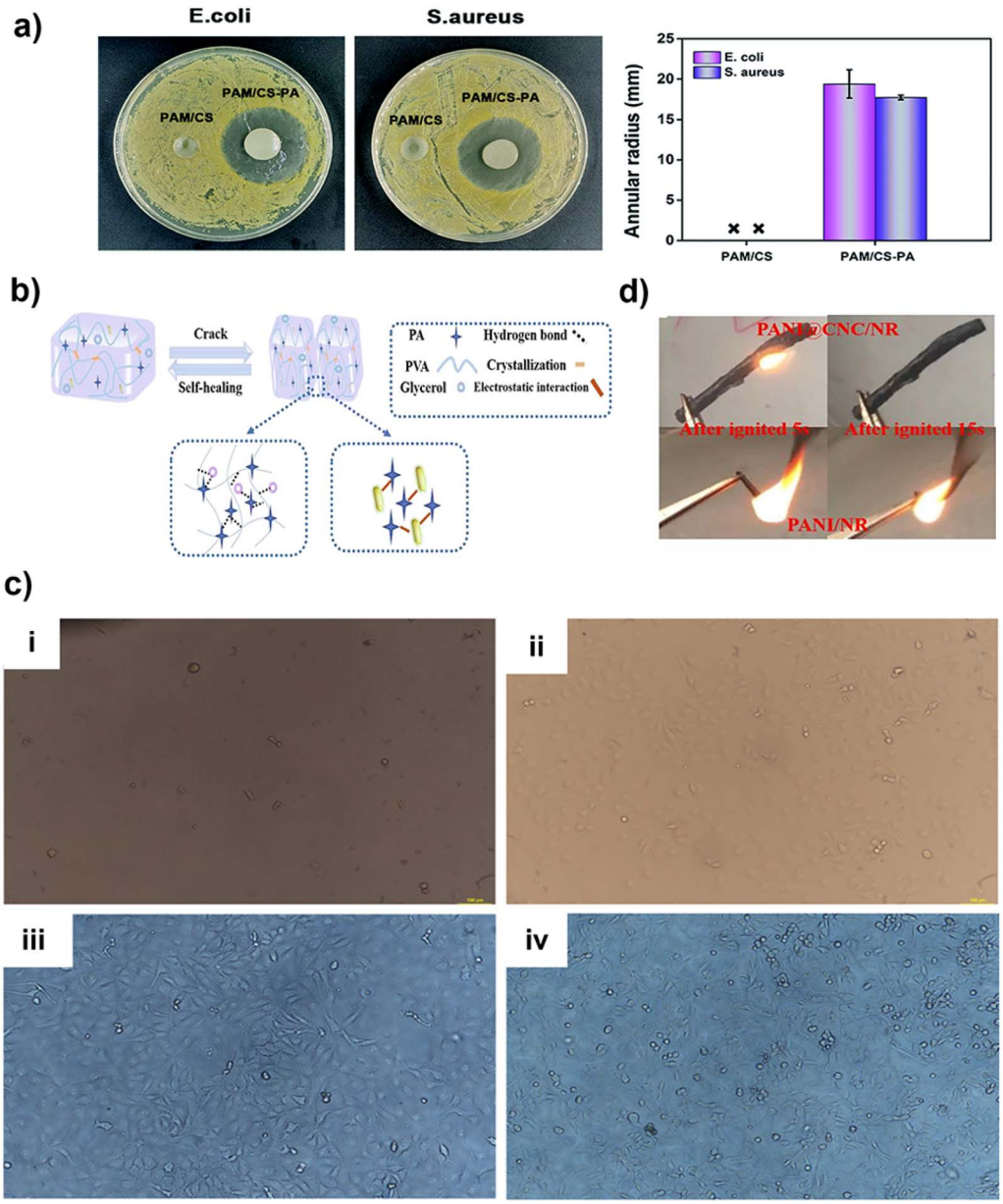

Fig. 18 (a) Antibacterial properties of PAM/CS hydrogels as a function of PA for strain sensors.[44] Copyright 2021, Royal Society of Chemistry. (b) Self-healing properties in poly(diallyldimethylammonium chloride) (PDDA) grafted onto a cellulose nanocrystals (CNCs)/PVA hydrogel using PA for strain sensors.[218] Copyright 2022, Elsevier. (c) Biocompatibility of PA hydrogels containing PVA/NH_2-POSS for strain sensors, cell-cultured for (i) 12 h, (ii) 24 h, (iii) 72 h, and (iv) 96 h.[216] Adapted with permission from ref. 216. Copyright 2020, American Chemical Society. (d) Flame retardant properties due to PA.[127] Copyright 2019, Elsevier.

networks endowed the hydrogel strain sensors with self-healing properties (Fig. 18(b)).[218] Similarly, conductive hydrogels containing PA composed of PVA and amino-polyhedral oligomeric silsesquioxane (NH_2-POSS) showed no apparent cytotoxicity to MDA-MB-231 cells, as shown in Fig. 18(c), suggesting the biocompatibility of PA in the hydrogels. In an *in vitro* cytotoxicity examination, the cells exhibited a spindle-like shape and increased cell number and growth rate on the surface of the hydrogels after 24, 72, and 96 h. No dead cells were observed.[216]

Moreover, PA is an environmentally friendly flame retardant. Zhang *et al.* developed PA-doped strain sensors that exhibited flame retardancy by self-extinguishing flame action within 20 s.[127]

Sorbitol

Sorbitol is a natural and important sugar alcohol, polyol-$C_6H_{14}O_6$ (molecular weight: 182.1 g mol^{-1}), comprising two primary and four secondary hydroxyl groups. It is commonly

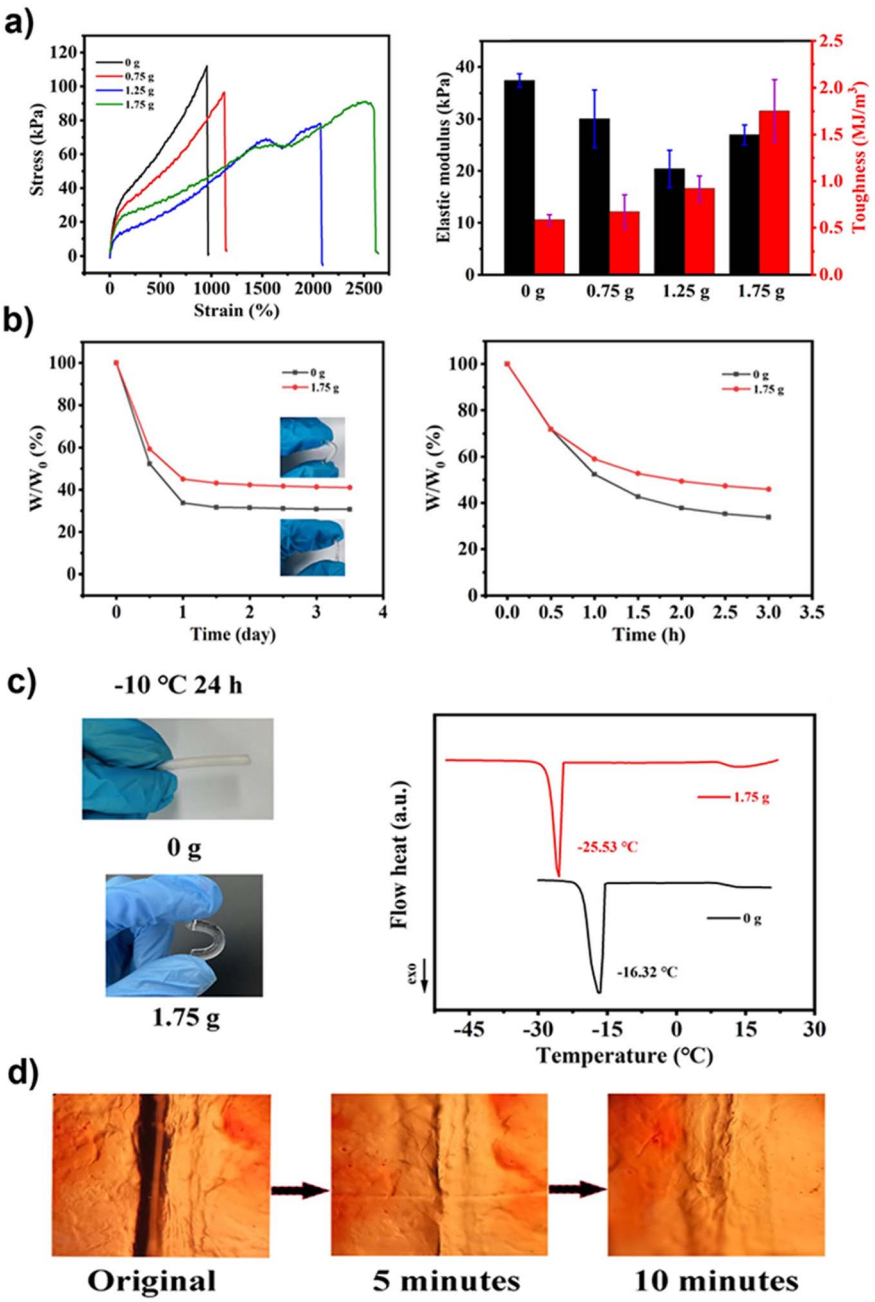

Fig. 19 (a) Effect of sorbitol on tensile stress–strain behavior and mechanical properties (elastic moduli and toughness) of the PAM/CS/D-sorbitol (PCS) conductive hydrogel for strain sensors, (b) water retention properties of the PCS hydrogel as a function of sorbitol at room temperature (left) and 50 °C (right), (c) anti-freezing properties as a function of sorbitol, and (d) self-healing properties (adapted from ref. 58). Copyright 2022, Elsevier.

found in fruit, corn, wheat starch, and cellulose. Sorbitol is extracted through polysaccharide decomposition and reduction. Sorbitol can be directly extracted using heterogeneous catalysts and hydrogenation reactions.[220,221] Sorbitol has been used in various biomedical applications, such as drug delivery vesicles,[222] bio-friendly carbon quantum dots for theragnostic,[223] and copolymerized network-based composites carrying biomaterials for bone regeneration.[224] In these applications, sorbitol exhibited no cytotoxic effects. Thus, sorbitol may be a better choice for developing hydrogel strain sensors.

Sorbitol performs various functions as a strain sensor in conductive hydrogels. For instance, Huang *et al.*[58] reported that sorbitol could have a plasticizing effect on hydrogels, exhibiting a decrease in the elastic modulus from 37 to 27 kPa, an increase in stretchability up to 2500%, and an increase in toughness up to 1.75 MJ m^{-3} (Fig. 19(a)). It was due to sorbitol that the hydrogels were moisturized for a long time, comparable at room temperature and 50 °C (Fig. 19(b)). Moreover, they were tolerant to freezing at subzero (−25 °C) temperatures, maintaining mechanical flexibility (Fig. 19(c)). Furthermore, sorbitol endowed the hydrogel with self-healing properties (Fig. 19(d)). Similar to sorbitol, other polyols, such as glycerol[94,95,225] and E_g,[125,226] in the presence of inorganic salts (such as sodium chloride, magnesium chloride, and aluminum chloride) are utilized in hydrogel-based strain sensors because of their excellent freezing resistance. Glycerol, a natural compound, comes from animal and plant sources and is commonly produced during the making of soap[227,228] and biodiesel[229,230] as a by-product, and thus has been considered a biomolecule.[231,232] The synthetic compound E_g is primarily produced through petrochemical processes, but attempts are being made to derive it from renewable resources such as biomass.[233–235]

Glycyrrhizic acid (GA)

Glycyrrhizic acid (GA), also known as glycyrrhizin (molecular weight: 822.9 g mol^{-1}), is a natural sweetener having an amphiphilic structure. It comprises two molecular parts: (i) the hydrophobic side of GA and (ii) the hydrophilic side of the diglucuronic unit with –OH and –COOH groups. Both the parts are connected by a glycosidic bond.[236,237] It is found in the roots and rhizomes of licorice plants.[238,239] Various methods for GA include solid phase extraction, microwave-assisted micellar extraction, microwave-assisted extraction, supercritical CO_2 extraction, and ultrasound-assisted extraction.[240,241]

GA can improve the mechanical properties of hydrogels. Zhang *et al.* described a hydrogel strain sensor composed of PVA/GA/AgNPs[242] (Fig. 20(a)), improving the mechanical properties of hydrogels for strain sensors. An improvement in the modulus of elasticity from 28 to 130 kPa, tensile strain from 300 to 500%, and toughness from 0.3 to 1.4 MJ m^{-3} was observed, as shown in Fig. 20(b). Moreover, GA *in situ* reduced Ag^+ ions to AgNPs (transparent appearance transformed into brownish color appearance) on the surface of hydrogels under UV light exposure for well-known antibacterial and UV-blocking effects, as shown in Fig. 20(c) and (d). However, it should be noted that GA itself was neither a UV-blocker nor a good antibacterial agent. The thickness of the AgNP layer on the surface increased with increasing UV exposure time to reduce the number of Ag^+ ions in the presence of GA, which improved the UV-blocking properties. Furthermore, the presence of GA in the hydrogel showed no cytotoxic effects, exhibiting a cell viability of 98% for HUVECs after 24 h and a favorable spindle cell morphology, as shown in Fig. 20(e).

Deoxyribose nucleic acid (DNA)-inspired molecules

Deoxyribose nucleic acid (DNA) is a long, complex molecule that stores and transmits genetic information.[243] It serves as a blueprint for life and provides instructions for the development and functioning of all living organisms.[244,245] The DNA molecule comprises two complementary strands that run in opposite directions and are held together by H bonds between nitrogenous bases. It consists of repeating units of four nitrogenous bases: adenine (A), guanine (G), cytosine (C), and thymine (T), and a sugar-phosphate backbone.[246,247] DNA acts as a polyacid over a wide pH range.[248]

DNA can be obtained from various sources, including cells such as blood cells, skin cells, hair follicles, tissues such as the liver or muscle tissue, microorganisms such as bacteria or viruses, and non-living sources such as bones, teeth, or hair.[249] There are 8–10 commonly used DNA extraction protocols.[250] The choice of the DNA extraction method depends on the state of the target DNA.[251] In terms of concentration, the Chelex method yielded the lowest amount of DNA, while the DNA IQ™ system, QIAGEN QIA cube, and QIAsymphony® DNA Investigator® Kit helped obtain the highest concentration of DNA.[252]

DNA is a macromolecule with a molecular weight greater than 5 Da. However, its building blocks, deoxyribose nucleotides, are small molecules with molecular weights less than 1 kDa.[253] DNA-inspired molecules such as deoxyribonucleotides (molecular weight < 1 kDa), including cytosine methacryloyl chloride,[254] acrylate adenine, thymine,[255,256] and adenosine monophosphate,[257] have been reported to improve the mechanical properties and adhesion of hydrogels to the skin. Zhang *et al.* reported that the H-forming ability of adenosine monophosphate molecules can increase the stretchability of hydrogels (Fig. 21(a) and (b)).[257] Furthermore, Kang *et al.* reported that adenine and thymine produced PAM/glycerol hydrogels with excellent self-healing properties (Fig. 21(c)).[255] The self-healing hydrogel showed excellent extensibility with a healing efficiency of 96.3% after 60 min of contact between cut halves of the hydrogel. In addition, the hydrogel strongly adhered to various substrates, including nonpolar polymers, polar polymers, metals, skin, and ceramics, as indicated in Fig. 21(d). Moreover, the presence of DNA-inspired nucleobases promoted biocompatibility in quaternized CS/PAM hydrogels (Fig. 21(e)).

Discussions

Citric acid (CA) in hydrogel-based strain sensors. The antibacterial effect of CA is due to the disruptive effect of the carboxyl groups on the bacterial cell membrane, which inhibits bacterial growth. CA ionizes by the transformation of the

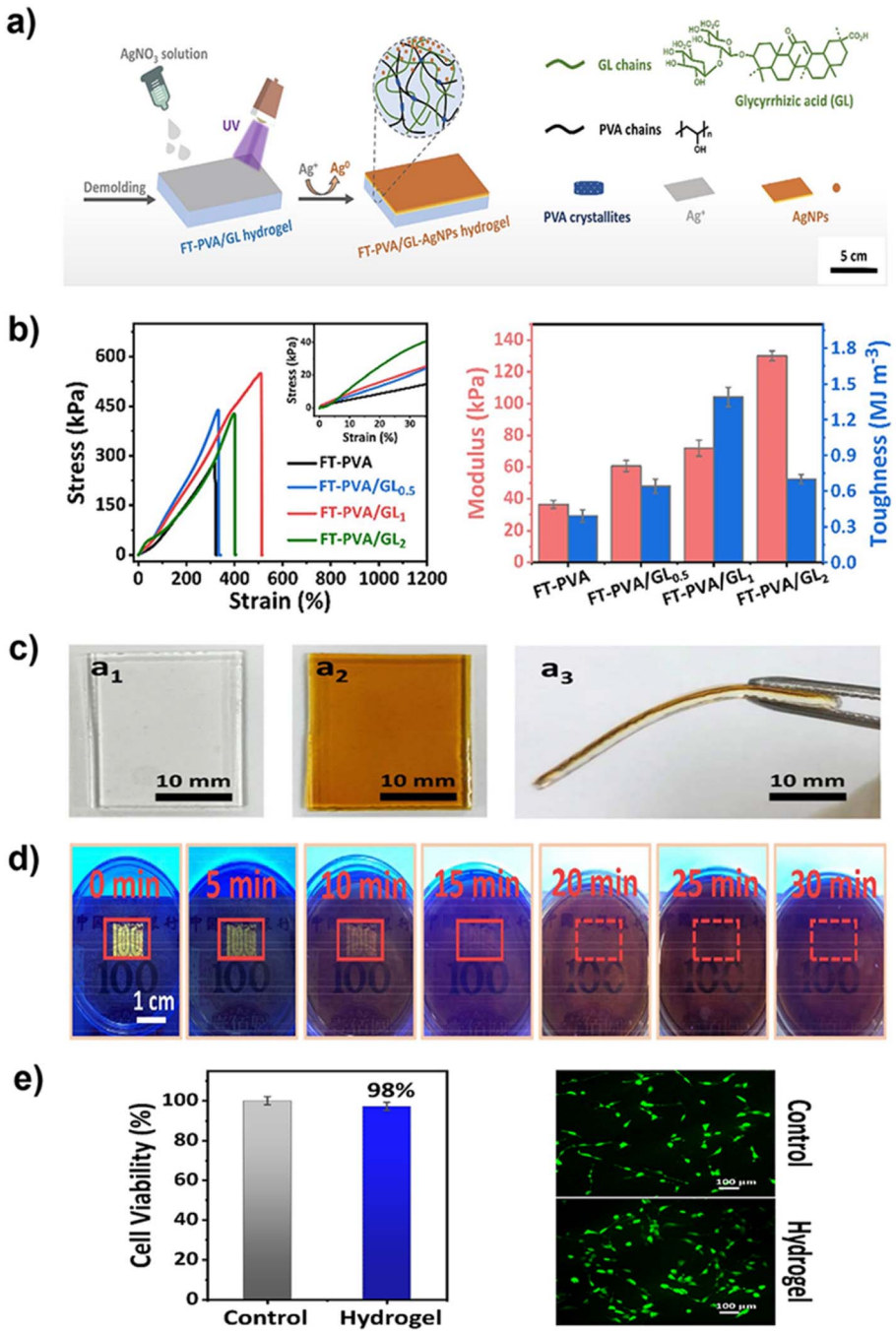

Fig. 20 (a) Schematic representation of the PVA/GA/Ag nanoparticle (AgNP) conductive hydrogel for strain sensors, (b) tensile stress–strain behavior and mechanical properties of hydrogels at various concentrations of GA, (c) *in situ* formation of the AgNP layer on the surface of hydrogels under the influence of UV radiation in the presence of GA, (d) UV-blocking properties of the PVA/GA/AgNP hydrogel, and (e) cell viability of the PVA/GA/AgNP hydrogel and morphology of cells on the surface of the hydrogels. Adapted with permission from ref 242. Copyright © 2021. Reprinted with permission from Elsevier B.V.

carboxyl groups (–COOH) into carboxylate groups ($–COO^-$) by losing H^+ (proton), which provides ionic conductivity in hydrogels for application as a piezoresistive strain sensor. Furthermore, the three carboxyl groups in CA can interact with functional groups in other hydrogel molecules through physical interactions, such as the formation of H bonds, electrostatic interactions, and covalent bonds, which provide hydrogels with a shape memory effect. The reported decrease in mechanical toughness with increasing CA concentration in the hydrogels may limit their applicability in strain sensors that require high mechanical stability. To harness the full potential of CA in strain sensing applications, future studies should focus on balancing its mechanical properties with other benefits. CA can impart adhesive properties to hydrogels owing to the interactions between the carboxyl groups of CA and the functional groups of various substrates. However, the optimal

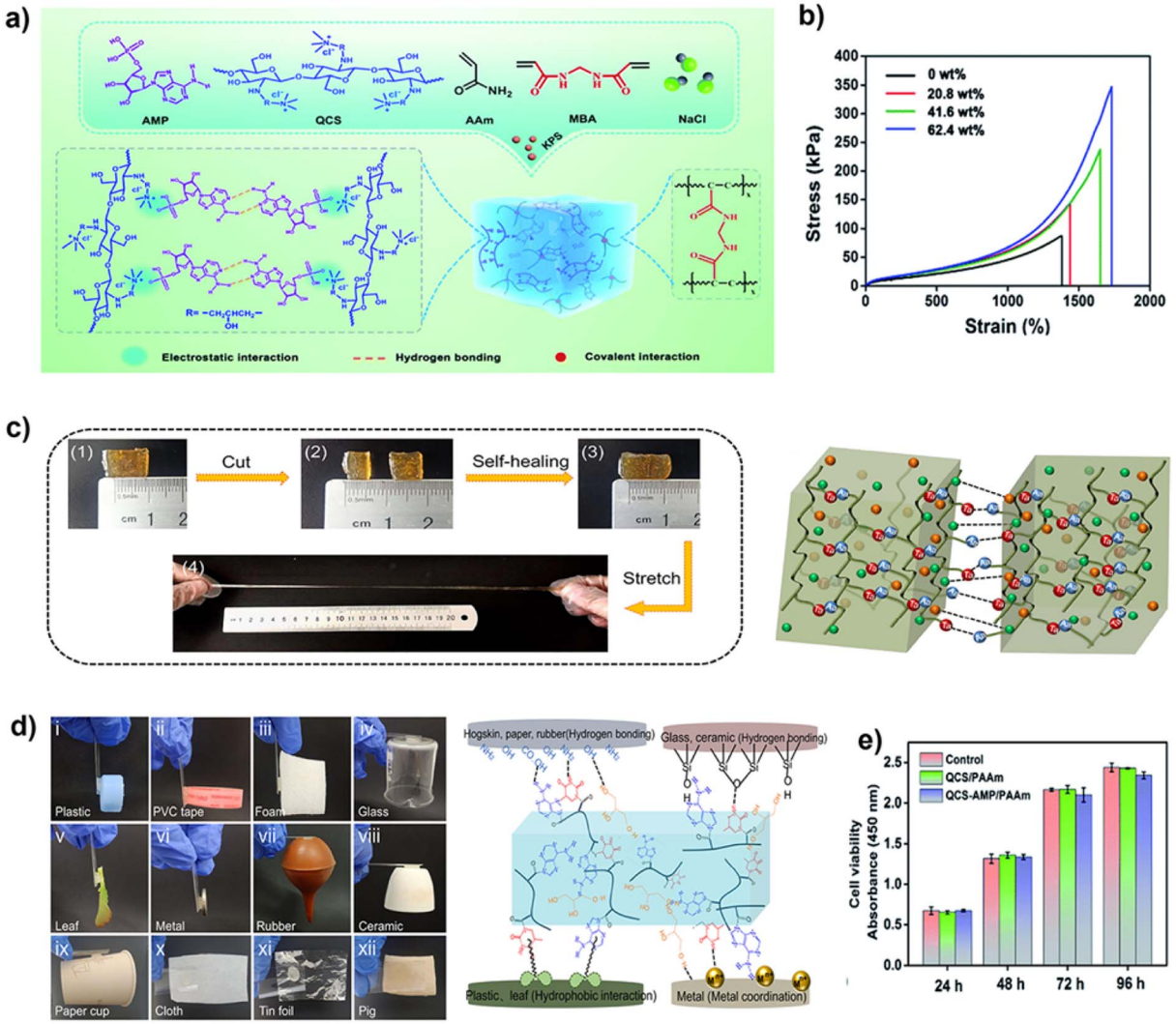

Fig. 21 (a) Schematic illustration of adenosine's ability to physically interact with polymer chains in a hydrogel network, forming a quaternized CS/PAM hydrogel for strain sensors and (b) tensile stress–strain behavior of quaternized CS/PAM hydrogels at various concentrations of adenosine.[257] Copyright 2021, Royal Society of Chemistry. Thymine and adenosine promote (c) self-healing and (d) adhesive properties in hydrogel strain sensors.[255] Adapted with permission from ref 255. Copyright 2022, American Chemical Society. (e) Biocompatibility of the quaternized CS/PAM hydrogel to strain sensors by increasing cell viability over various time periods.[257] Copyright 2021, Royal Society of Chemistry.

concentration must be identified to ensure adequate adhesion without compromising mechanical strength and flexibility. The reduction of Ag^+ to AgNPs in the hydrogels was due to the ability of ionized CA molecules with negatively charged carboxylate ions ($–COO^-$) to donate electrons to reduce Ag^+ to AgNPs. The strain-sensing mechanism can be explained by the fact that the presence of CA ensured uniform dispersion of AgNPs in the matrix of the hydrogel strain sensor, forming conductive paths. When stretched and released, the conductive paths are broken and rebuilt, thereby supporting the conduction mechanism of piezoresistive-type strain sensing. Although the mechanism of strain sensing using CA is well understood, understanding how the CA content variation can tune the performance indicators of hydrogel strain sensors, such as their sensitivity, linearity, and response time, requires further studies. The effect of CA on long-term stability in terms of the retention of mechanical properties should also be determined using a proper study plan.

Zwitterionic osmolytes in hydrogel-based strain sensors. The high resistance to non-specific protein absorption supports biocompatibility owing to the high hydrophilicity of betaine moieties. The antifouling properties were attributed to the improved retention of water molecules on the surface of the hydrogel due to the excellent hydrophilicity of proline molecules that resist the non-specific absorption of proteins. Biocompatible proline promotes wound healing, attributed to the intrinsic ability of proline to accelerate collagen formation in the skin after attaching to wounded tissues. Freezing tolerance is attributed to the ability of betaine and proline molecules to interact with water molecules at subzero temperatures, resisting in H bonding among water molecules, which prevents

ice formation. Mechanical properties such as stretchability (~1800%), elastic moduli, and toughness are improved due to the $-NH_2^+$ site of proline that forms H bonds with the $-COO^-$ groups of GG polymer chains. Improvement in the adhesive properties of the hydrogel was observed for skin and other substrates due to the zwitterionic nature of these molecules that causes the hydrogels to interact with both negatively and positively charged functional groups on the skin and other substrates. Despite the potential benefits of using zwitterionic osmolytes as hydrogel strain sensors, some gaps remain to be addressed. A critical challenge is that zwitterionic osmolytes can have a plasticizing effect on hydrogel mechanics, and detailed studies to understand such behavior are lacking. Additionally, the effects of zwitterionic osmolytes on the sensitivity and sensing behavior have not been thoroughly investigated beyond their use in piezoresistive hydrogel-based strain sensors. It would be valuable to explore the potential of zwitterionic osmolytes in other types of strain sensors, such as capacitive strain sensors, which rely on their dielectric properties.[258] Furthermore, zwitterionic osmolytes and salt electrolytes have been used together in hydrogel strain sensors. However, there is a gap in determining how their interactions can impact the sensing properties.[259]

Tannic acid (TA) in hydrogel-based strain sensors. TA improves the mechanical properties of gelatin hydrogels because the –OH groups and benzene rings in the polyphenolic moieties of TA can crosslink gelatin polymer chains through H bonds and hydrophobic interactions. TA improves the gelation rate *via* radical polymerization because the catechol groups on TA and the Fe^{3+} ions in the hydrogel monomer system quickly activate sodium persulfate for free-radical polymerization, forming PAA/TA@hemicellulose/Fe^{3+} hydrogels. TA endows hydrogels with UV-blocking properties because TA contains several aromatic rings in its chemical structure, which can absorb UV radiation, making it an effective blocker of UV light. Therefore TA is used in wearable hydrogel strain sensors to protect the skin from the harmful effects of UV radiation. The antibacterial activity of TA in hydrogels is attributed to the affinity of the phenolic sites of TA for the bacterial surface, including protein sites, which destabilize the bacterial cell membrane and inhibit further bacterial growth.[260,261] Polyphenolic catechol groups on TA molecules induce self-healing properties in hydrogels by forming dynamic H bonds that reconnect the broken bonds of –COOH and $-NH_2$ groups on silk fibroin polymer chains, –OH groups on PVA, and coordination with borate ions. The moderate TA content in hydrogels provides biocompatibility, which is attributed to the potent antioxidant properties of TA that enable it to counteract reactive oxygen species and other free radicals that initiate oxidative stress, leading to harm to cells and tissues.[38,262] Therefore, TA can protect cells and tissues from oxidative injury, highlighting its biocompatibility. The tunability of conductivity and sensitivity can be attributed to the release of Cl^- ions from the gelatin polymer chains and the partial de-crosslinking of citrate ions within the gel network upon crosslinking with TA. This explanation also accounts for the observed microstructural changes, which involve a concurrent increase in both the pore size and pore wall thickness, ultimately resulting in a reduced modulus and enhanced toughness. TA has enabled researchers to adjust strain sensitivity. However, certain limitations and challenges must be considered, such as difficulties in scaling up the use of high TA content owing to the limited solubility and rapid crosslinking of TA in aqueous systems with polymers.[192] The long-term stability of hydrogels and their strain-sensing performance may be affected by the interactions between TA and salt electrolytes, which should be studied in detail.[263] Most TA-based hydrogel strain sensors operate *via* piezoresistive mechanisms. The potential of TA in other types of strain-sensing mechanisms should also be determined.

Phytic acid (PA) in hydrogel-based strain sensors. Lu *et al.* reported that the oxygen in the dihydrogen phosphate moieties of PA forms H bonds with the H in the –OH groups of PVA,[217,264] the –COOH groups of PAA,[219] or the $-NH_2$ groups of PAM and polyaniline[121,265–267] contributing to physical cross-linking in the hydrogel networks. The ability of PA to provide hydrogels with ionic conductivity is attributed to its acidic nature, which donates H^+ ions to the aqueous phase of the hydrogels. The freezing tolerance of PA-containing hydrogels is attributed to the formation of H bonds between a large number of electronegative oxygen sites on the PA molecule and the electropositive H atoms on water molecules at subzero temperatures. The same phenomenon accounts for the dehydration resistance of PA-containing hydrogels, which decreases the vapor pressure of water from hydrogels, but in relatively high humidity environments (75%) at room temperature.[44,268] PA combines toughness and reusability through thermoplasticity owing to the physical cross-linking forces of PA with polymer chains in the hydrogel network. The excellent PA-based physical crosslinking provided a uniform and fast transfer of the load across the polymer network in the hydrogel, which resulted in a wide linear working range and a fast response for strain sensing. The antibacterial activity of PA-containing hydrogels is attributed to the chelating properties of PA with Ca^{2+} and Mg^{2+} ions or the release of H^+ ions that damage the bacterial membrane.[44,268] Although no cytotoxicity was found in the PA-based hydrogels, which might be due to their inherent natural origin, more studies are required to confirm the biocompatibility of hydrogels containing PA. The flame retardancy of PA-containing hydrogels is due to the phosphorus-rich groups of PA, which produce $PO^{\bullet}$ radicals that have a quenching effect on the combustion reactions.[126,127]

Sorbitol in hydrogel-based strain sensors. Sorbitol has a plasticizing effect on hydrogels owing to the interaction of the –OH groups of sorbitol with the hydrogel constituents. The dehydration resistance and freezing tolerance of the hydrogel are attributed to the –OH groups of sorbitol, which form strong H bonds with water molecules. Furthermore, the –OH groups of sorbitol can interact with the polar functional groups of the hydrogel constituents, forming reversible noncovalent interactions for self-healing properties. The mechanisms underlying the roles of sorbitol are well explained. However, conducting further research to confirm these findings across various hydrogel compositions and in practical applications is essential.

Glycyrrhizic acid (GA) in hydrogel-based strain sensors. The improvement in the mechanical properties of the hydrogel was attributed to the ability of GA to self-assemble in a glycerol/water binary solvent and form H bonds with other polar functional groups (–OH groups) on PVA. Although we concluded that GA could suppress the cytotoxic effects of AgNPs, the underlying mechanism was not discussed. Further studies are required to confirm these findings.

Deoxyribose nucleic acid (DNA)-inspired molecules. The building blocks of DNA, deoxyribose nucleotides, improve the mechanical properties, self-healing properties, and adhesion of hydrogels to the skin. These improvements were attributed to the strong H bond-forming ability of the nucleobases. The mechanisms underlying these characteristics are well established. Furthermore, these nucleobases promote biocompatibility in hydrogels because of their inherent biocompatibility[257] and capacity to modulate cellular interactions through ligand binding.[269,270] Although incorporating DNA-inspired molecules into hydrogels has shown promising results, further research is required to optimize their use in different hydrogel compositions, investigate their long-term stability, and improve their mechanical toughness without compromising their adhesion properties.

Conclusion and perspectives

Conclusion

In recent years, various functional properties have been incorporated into hydrogels to facilitate their practical implementation as strain sensors in various applications, such as human health monitoring, robotic smart skins, and human–machine interfaces, considering the longevity of the functionality and the quality of the strain-sensing performance. Notably, rapid advancements have been made in the operational quality of hydrogel-based strain sensors through the extensive assessment of performance indicators, including a wide linear working range, sensitivity, response/recovery time, and reduced hysteresis. Although the four fundamental strain-sensing mechanisms—piezoresistivity, capacitance, piezoelectricity, and triboelectricity—are well established, sensors that employ multiple mechanisms are now available, broadening the range of potential applications for strain sensors. Furthermore, we examined the incorporation of small biomolecules to enhance the functional properties of the hydrogels used in strain sensors. Small biomolecules offer numerous advantages for developing hydrogel-based strain sensors with multifunctional capabilities that cannot be achieved solely by employing polymer networks in their native states within hydrogels. This strategy also eliminates the reliance on less accessible methods to induce multiple functionalities. Polyacids, such as TA, PA, and DNA-inspired molecules, possess functional groups that significantly improve the mechanical properties of hydrogels by reinforcing physical interactions such as H bonding, ionic interactions, and hydrophobic interactions within the hydrogel network. The functional groups of polyacids and sorbitol enhance self-healing capabilities and increase adhesion to various substrates, including the skin, making these hydrogels suitable for wearable devices. TA accelerates the gelation rate by promoting radical polymerization and forming synthetic polymer networks in hydrogels. GA converts metal ions into metallic NPs, such as transforming Ag^{+} into AgNPs, endowing the hydrogels with additional functionalities. The robust coordination of PA and zwitterionic osmolytes with water contributes to exceptional freezing tolerance and preserves the hydrogel function at subzero temperatures. The highly hydrophilic nature of zwitterionic osmolytes also imparts antifouling properties to hydrogel surfaces. PA further reduced the dehydration rate of the hydrogels, extending their functional lifespan and providing flame retardancy. The ionizable nature of CA and PA allows the modulation of ionic conductivity in hydrogels and imparts remarkable antibacterial properties. The discussed biomolecules ensured the biocompatibility of the hydrogels. From the perspective of the performance indicators of the hydrogel-based strain sensor, only TA and PA were found to affect the strain-sensing performance.

Perspectives

It is expected that the use of small biomolecules will continue to be of great interest in developing hydrogel-based strain sensors. However, several challenges must be addressed in the field of hydrogel-based strain sensors and small biomolecules.

Developing hydrogel-based strain sensors for multiple applications with multifunctional properties. The application-specific functionality and strain-sensing performance of hydrogel-based strain sensors are well documented in the existing literature. However, the field has reached a saturation point. To foster further growth, future research should concentrate on creating hydrogel compositions that exhibit multifunctional properties for various applications. For example, recent studies have reported the achievement of dual-sensing modes for multiple applications, such as piezoresistive and piezoelectric modes.[83,106] However, these sensors often lack essential multifunctional properties for long-lasting operation, including freezing tolerance and dehydration resistance. Therefore, the incorporation of multifunctional small biomolecules into the development of hydrogel-based dual-mode strain sensors should be attempted in the future to achieve longevity and multifunctional properties, which would increase the practical adaptability of hydrogel-based strain sensors.

Focusing on improving the performance indicators of multifunctional hydrogel-based strain sensors. Enhancing the key performance indicators of hydrogel-based strain sensors, including broad strain range, linearity, high sensitivity, rapid response/recovery time, and low hysteresis, is essential for practical adaptation to a wide range of applications. While most studies on hydrogel strain sensors have optimized the hydrogel conditions based on mechanical and functional properties, there has been less emphasis on gaining insights into fine-tuning these performance indicators for hydrogel strain sensors.[51,271,272] Future research should address this aspect by providing more comprehensive experimental details and strategies to optimize these crucial performance indicators.

Recent studies have demonstrated that incorporating small biomolecules into hydrogels can successfully impart

multifunctional properties such as mechanical robustness, self-healing, freezing tolerance, and dehydration resistance. However, the majority of small biomolecule-integrated hydrogel-based strain sensors operate primarily *via* piezoresistive sensing mechanisms, which may significantly limit their range of applications. In this regard, a potential future research direction should focus on broadening the scope of their use to multiple applications. For instance, introducing piezoelectric nanomaterials into hydrogel networks incorporating small biomolecules using a composite hydrogel approach can produce a dual-sensing mode, thus enhancing their scope of application.

Addressing the tradeoff between multifunctional properties in small biomolecule-integrated hydrogel-based strain sensors. Stretchability, toughness, and self-adhesion are attractive features of hydrogels for use in mechanically stable wearable strain sensors. Polyacids, including TA and DNA, regulate the cohesive and adhesive properties. However, close optimization is required to achieve a balance between cohesion and adhesion, limiting the simultaneous improvement of both cohesion and adhesion. In this scenario, the challenge is to achieve high cohesion and adhesion simultaneously to extend the practical applications of tough and adhesive strain sensors.

Optimizing the electrochemical properties of small biomolecule-integrated hydrogels for enhanced piezoresistive strain sensing performance across wide temperature ranges. In piezoresistive strain sensors, small biomolecules such as sorbitol and zwitterionic osmolytes have been shown to enhance the freezing tolerance of hydrogels, allowing them to maintain functionality at subzero temperatures. Hydrogels are selected for strain-sensing applications based on optimizing their mechanical properties. However, the large molecular size and polar nature of these small biomolecules may influence the mobility of free ions, potentially reducing ionic conductivity in certain cases.[172,178] Therefore, it is crucial to investigate this potential effect on the electrochemical properties of hydrogels intended for strain sensing across a wide temperature range, from room temperature to subzero temperatures, to understand the underlying mechanisms better and bolster their practical adaptability. Moreover, future research should focus on selecting hydrogels for strain-sensing applications by optimizing their electrochemical properties in detail, considering the performance indicators of hydrogel-based strain sensors and mechanical considerations.

Expanding dehydration resistance in small biomolecule-based hydrogel strain sensors for diverse humidity environments. On a broader scale, small biomolecules, such as PA and sorbitol, impart dehydration resistance to hydrogels and prolong their functional lifespan. Resistance to dehydration is highly dependent on the relative humidity of the surrounding environment. Researchers have reported the dehydration resistance of biomolecule-based hydrogel strain sensors in environments with relative humidity above 50%.[44,45] However, these humidity conditions are not universal. Therefore, dehydration resistance should be reported over a wide range of humidity environments.

Author contributions

Syed Farrukh Alam Zaidi: conceptualization, data curation, formal analysis, methodology, visualization, and writing-original draft. Aiman Saeed: data curation, formal analysis, visualization, and writing-review & editing. Jun Hyuk Heo: conceptualization, investigation, validation, and writing-review & editing. Jung Heon Lee: conceptualization, funding acquisition, investigation, resources, supervision, validation, and writing-review & editing.

Conflicts of interest

There are no conflicts to declare.

Acknowledgements

This study was supported by the National Research Foundation (NRF) of Korea for the Basic Science Research Program funded by the Ministry of Education (NRF-2019R1A6A1A03033215 and 2022R1C1C2002823), and the Ministry of Science and ICT (NRF-2020R1A2C2006100).

Notes and references

1 H. Chen, F. Zhuo, J. Zhou, Y. Liu, J. Zhang, S. Dong, X. Liu, A. Elmarakbi, H. Duan and Y. Fu, *Chem. Eng. J.*, 2023, **464**, 142576.
2 A. Yadav, N. Yadav, Y. Wu, S. RamaKrishna and Z. Hongyu, *Adv. Mater.*, 2023, **4**, 1444–1459.
3 Z. Duan, Y. Jiang, Q. Huang, Q. Zhao, Z. Yuan, Y. Zhang, S. Wang, B. Liu and H. Tai, *J. Mater. Chem. C*, 2021, **9**, 14003–14011.
4 X. Qi, P. Matteini, B. Hwang and S. Lim, *Cellulose*, 2023, **30**, 1543–1552.
5 Z. Duan, Z. Yuan, Y. Jiang, L. Yuan and H. Tai, *J. Mater. Chem. C*, 2023, **11**, 5585–5600.
6 X. Li, H. Sun, R. He, Y. Liu and Q. Wang, *Chem. Eng. J.*, 2023, **458**, 141535.
7 Z. Duan, Y. Jiang, S. Wang, Z. Yuan, Q. Zhao, G. Xie, X. Du and H. Tai, *ACS Sustainable Chem. Eng.*, 2019, **7**, 17474–17481.
8 Q. Huang, Y. Jiang, Z. Duan, Z. Yuan, B. Liu, Q. Zhao, Y. Zhang, Y. Sun, P. Sun and H. Tai, *J. Phys. D: Appl. Phys.*, 2021, **54**, 284003.
9 H. Tai, Z. Duan, Y. Wang, S. Wang and Y. Jiang, *ACS Appl. Mater. Interfaces*, 2020, **12**, 31037–31053.
10 L. Shen, S. Zhou, B. Gu, S. Wang and S. Wang, *Adv. Eng. Mater.*, 2023, 2201882.
11 X. Yao, S. Zhang, L. Qian, N. Wei, V. Nica, S. Coseri and F. Han, *Adv. Funct. Mater.*, 2022, **32**, 2204565.
12 Z. Shen, Z. Zhang, N. Zhang, J. Li, P. Zhou, F. Hu, Y. Rong, B. Lu, G. Gu, Z. Shen, N. Zhang, J. Li, P. Zhou, Y. Rong, G. Gu, Z. Zhang, F. Hu and B. Lu, *Adv. Mater.*, 2022, **34**, 2203650.

13 L. Hu, Y. Xie, S. Gao, X. Shi, C. Lai, D. Zhang, C. Lu, Y. Liu, L. Du, X. Fang, F. Xu, C. Wang and F. Chu, *Carbohydr. Polym.*, 2023, **312**, 120827.
14 S. R. Montoro, S. de F. Medeiros and G. M. Alves, *Nanostruct. Polym. Blends*, 2014, 325–355.
15 S. F. A. Zaidi, A. Saeed, V.-C. Ho, J. H. Heo, H. H. Cho, N. Sarwar, N.-E. Lee, J. Mun and J. H. Lee, *Int. J. Biol. Macromol.*, 2023, **234**, 123725.
16 E. G. Kifaro, M. J. Kim, S. Jung, J. Y. Noh, C. S. Song, G. Misinzo and S. K. Kim, *BioChip J.*, 2022, **16**, 409–421.
17 N. Gao and H. You, *BioChip J.*, 2021, **15**, 23–41.
18 I. C. Carvalho, *Mater. Sci. Eng., C*, 2017, **78**, 690–705.
19 F. S. Tenório, T. L. do Amaral Montanheiro, A. M. I. dos Santos, M. dos Santos Silva, A. P. Lemes and D. B. Tada, *J. Appl. Polym. Sci.*, 2021, **138**, 49819.
20 F. Ding, Y. Dong, R. Wu, L. Fu, W. Tang, R. Zhang, K. Zheng, S. Wu and X. Zou, *New J. Chem.*, 2022, **46**, 11676–11684.
21 W. Zhang, L. Xu, M. Zhao, Y. Ma, T. Zheng and L. Shi, *Soft Matter*, 2022, **18**, 1644–1652.
22 P. Deng, L. Yao, J. Chen, Z. Tang and J. Zhou, *Carbohydr. Polym.*, 2022, **276**, 118718.
23 S. H. Kim, B. Lee, J. H. Heo, K. E. Lee, P. Shankar, K. H. Han and J. H. Lee, *Part. Part. Syst. Charact.*, 2019, **36**, 1800292.
24 S. Y. Chin, S. Shahruddin, G. K. Chua, N. Samsodin, H. D. Setiabudi, N. S. Karam Chand, F. N. Chew, J. X. Leong, R. Jusoh and N. A. Samsudin, *ACS Sustainable Chem. Eng.*, 2021, **9**, 6510–6533.
25 G. Ghosh, A. Bag, A. Hanif, M. Meeseepong, Y. R. Lee, N.-E. Lee, G. Ghosh, A. Bag, A. Hanif, Y. R. Lee, N.-E. Lee and M. Meeseepong, *Adv. Funct. Mater.*, 2023, **33**, 2209277.
26 G. Ghosh, M. Meeseepong, A. Bag, A. Hanif, M. V. Chinnamani, M. Beigtan, Y. Kim and N. E. Lee, *Mater. Today*, 2022, **57**, 43–56.
27 S. Yoon, B. Lee, C. Kim, J. H. Chang, M. J. Kim, H. Bin Bae, K. E. Lee, W. K. Bae and J. H. Lee, *Chem. Mater.*, 2021, **33**, 5257–5267.
28 K.-I. Kim, S. Yoon, J. Chang, S. Lee, H. Hun Cho, S. Hwan Jeong, K. Jo, J. Heon Lee, K. Kim, J. Chang, S. H. Jeong, J. H. Lee, S. Yoon, H. H. Cho, S. Lee and K. Jo, *Small*, 2020, **16**, 1905821.
29 S. H. Jeong, C. H. Park, H. Song, J. H. Heo and J. H. Lee, *J. Clean. Prod.*, 2022, **368**, 133241.
30 S. H. Jeong, J. H. Heo, J. W. J. H. Lee, M. J. Kim, C. H. Park and J. W. J. H. Lee, *ACS Appl. Mater. Interfaces*, 2021, **13**, 22935–22945.
31 M. Kumorek, I. M. Minisy, T. Krunclová, M. Voršiláková, K. Venclíková, E. M. Chánová, O. Janoušková and D. Kubies, *Mater. Sci. Eng., C*, 2020, **109**, 110493.
32 H. El Gharras, *Int. J. Food Sci. Technol.*, 2009, **44**, 2512–2518.
33 A. E. Hagerman and C. T. Robbins, *J. Chem. Ecol.*, 1987, **13**, 1243–1259.
34 A. M. Hashim, B. M. Alharbi, A. M. Abdulmajeed, A. Elkelish, H. M. Hassan and W. N. Hozzein, *Plants*, 2020, **9**, 869.
35 G. P. Chung, C. L. Kyu, W. L. Dong, Y. C. Ho and P. J. Albert, *J. Chem. Ecol.*, 2004, **30**, 2269–2283.
36 J. S. Martin, M. M. Martin and E. A. Bernays, *J. Chem. Ecol.*, 1987, **13**, 605–621.
37 G. Sharifzadeh and H. Hosseinkhani, *Adv. Healthcare Mater.*, 2017, **6**, 1700801.
38 N. Sahiner, S. Sagbas, M. Sahiner, C. Silan, N. Aktas and M. Turk, *Int. J. Biol. Macromol.*, 2016, **82**, 150–159.
39 H. Fan, L. Wang, X. Feng, Y. Bu, D. Wu and Z. Jin, *Macromolecules*, 2017, **50**, 666–676.
40 P. Li, Y. Sui, X. Dai, Q. Fang, H. Sima and C. Zhang, *Macromol. Biosci.*, 2021, **21**, 2100055.
41 J. Jing, S. Liang, Y. Yan, X. Tian and X. Li, *ACS Biomater. Sci. Eng.*, 2019, **5**, 4601–4611.
42 L. Zhao, Z. Ren, X. Liu, Q. Ling, Z. Li and H. Gu, *ACS Appl. Mater. Interfaces*, 2021, **13**, 11344–11355.
43 S. Ko, A. Chhetry, D. Kim, H. Yoon and J. Y. Park, *ACS Appl. Mater. Interfaces*, 2022, **14**, 31363–31372.
44 Q. Zhang, X. Liu, J. Zhang, L. Duan and G. Gao, *J. Mater. Chem. A*, 2021, **9**, 22615–22625.
45 C. Liu, R. Zhang, Y. Wang, J. Qu, J. Huang, M. Mo, N. Qing and L. Tang, *J. Mater. Chem. A*, 2023, **11**, 2002–2013.
46 Z. Qin, X. Sun, H. Zhang, Q. Yu, X. Wang, S. He, F. Yao and J. Li, *J. Mater. Chem. A*, 2020, **8**, 4447–4456.
47 D. Hardman, T. George Thuruthel and F. Iida, *NPG Asia Mater.*, 2022, **14**, 1–13.
48 X. Jing, X. Y. Wang, H. Y. Mi and L. S. Turng, *Mater. Lett.*, 2019, **237**, 53–56.
49 J. W. Lee, S. Chae, S. Oh, D. H. Kim, S. H. Kim, S. J. Kim, J. Y. Choi, J. H. Lee and S. Y. Song, *Adv. Healthcare Mater.*, 2023, **12**, 2201665.
50 S. H. Kim, S. Oh, S. Chae, J. W. Lee, K. H. Choi, K. E. Lee, J. Chang, L. Shi, J. Y. Choi and J. H. Lee, *Nano Lett.*, 2019, **19**, 5717–5724.
51 S. F. A. Zaidi, Y. A. Kim, A. Saeed, N. Sarwar, N.-E. E. Lee, D. H. Yoon, B. Lim and J. H. Lee, *Int. J. Biol. Macromol.*, 2022, **209**, 1665–1675.
52 J. Wang, F. Tang, Y. Wang, Q. Lu, S. Liu and L. Li, *ACS Appl. Mater. Interfaces*, 2020, **12**, 1558–1566.
53 H. Zhang, X. Wang, L. Wang, T. Sun, X. Dang, D. King and X. You, *Soft Matter*, 2021, **17**, 9399–9409.
54 J. Li, Z. Yang, Z. Jiang, M. Ni and M. Xu, *Int. J. Biol. Macromol.*, 2022, **209**, 1975–1984.
55 X. Sun, M. Yao, S. He, X. Dong, L. Liang, F. Yao, J. Li, X. Sun, M. Yao, S. He, X. Dong, L. Liang, F. Yao and J. Li, *Adv. Mater. Technol.*, 2022, **7**, 2101283.
56 J. Yin, C. Lu, C. Li, Z. Yu, C. Shen, Y. Yang, X. Jiang and Y. Zhang, *Composites, Part B*, 2022, **230**, 109528.
57 Q. Jiao, L. Cao, Z. Zhao, H. Zhang, J. Li and Y. Wei, *Biomacromolecules*, 2021, **22**, 1220–1230.
58 C. Huang, Q. Miao, Z. He, P. Fan, Y. Chen, Q. Zhang, X. He, L. Li and X. Liu, *Eur. Polym. J.*, 2022, **172**, 111240.
59 X. Lv, S. Tian, C. Liu, L. L. Luo, Z. B. Shao and S. L. Sun, *Eur. Polym. J.*, 2021, **160**, 110779.
60 M. Pan, M. Wu, T. Shui, L. Xiang, W. Yang, W. Wang, X. Liu, J. Wang, X. Z. Chen and H. Zeng, *J. Colloid Interface Sci.*, 2022, **622**, 612–624.
61 E. M. Stewart, S. Narayan and L. Anand, *J. Mech. Phys. Solids*, 2023, **173**, 105196.

62 M. Guo, X. Yang, J. Yan, Z. An, L. Wang, Y. Wu, C. Zhao, D. Xiang, H. Li, Z. Li and H. Zhou, *J. Mater. Chem. A*, 2022, **10**, 16095–16105.
63 Z. Xie, Z. Chen, X. Hu, H. Y. Mi, J. Zou, H. Li, Y. Liu, Z. Zhang, Y. Shang and X. Jing, *J. Mater. Chem. C*, 2022, **10**, 8266–8277.
64 C. Z. Hang, X. F. Zhao, S. Y. Xi, Y. H. Shang, K. P. Yuan, F. Yang, Q. G. Wang, J. C. Wang, D. W. Zhang and H. L. Lu, *Nano Energy*, 2020, **76**, 105064.
65 H. Zhang, D. Zhang, Z. Wang, G. Xi, R. Mao, Y. Ma, D. Wang, M. Tang, Z. Xu and H. Luan, *ACS Appl. Mater. Interfaces*, 2023, **15**, 5128–5138.
66 K. Meng, X. Xiao, W. Wei, G. Chen, A. Nashalian, S. Shen, X. Xiao and J. Chen, *Adv. Mater.*, 2022, **34**, 2109357.
67 J. Lin, R. Fu, X. Zhong, P. Yu, G. Tan, W. Li, H. Zhang, Y. Li, L. Zhou and C. Ning, *Cell Rep. Phys. Sci.*, 2021, **2**, 100541.
68 G. Lin, M. Si, L. Wang, S. Wei, W. Lu, H. Liu, Y. Zhang, D. Li, T. Chen, G. Lin, L. Wang, M. Si, S. Wei, W. Lu, H. Liu, Y. Zhang, D. Li and T. Chen, *Adv. Opt. Mater.*, 2022, **10**, 2102306.
69 H. Zhou, Z. Wang, W. Zhao, X. Tong, X. Jin, X. Zhang, Y. Yu, H. Liu, Y. Ma, S. Li and W. Chen, *Chem. Eng. J.*, 2021, **403**, 126307.
70 X. J. Zha, S. T. Zhang, J. H. Pu, X. Zhao, K. Ke, R. Y. Bao, L. Bai, Z. Y. Liu, M. B. Yang and W. Yang, *ACS Appl. Mater. Interfaces*, 2020, **12**, 23514–23522.
71 H. Wu, H. Qi, X. Wang, Y. Qiu, K. Shi, H. Zhang, Z. Zhang, W. Zhang and Y. Tian, *J. Mater. Chem. C*, 2022, **10**, 8206–8217.
72 J. Hu, Y. Wu, Q. Yang, Q. Zhou, L. Hui, Z. Liu, F. Xu and D. Ding, *Carbohydr. Polym.*, 2022, **275**, 118697.
73 X. Pei, H. Zhang, Y. Zhou, L. Zhou and J. Fu, *Mater. Horiz.*, 2020, **7**, 1872–1882.
74 H. Jiang, N. M. Carter, A. Zareei, S. Nejati, J. F. Waimin, S. Chittiboyina, E. E. Niedert, T. Soleimani, S. A. Lelièvre, C. J. Goergen and R. Rahimi, *ACS Appl. Bio Mater.*, 2020, **3**, 4012–4024.
75 S. Xia, S. Song, F. Jia and G. Gao, *J. Mater. Chem. B*, 2019, **7**, 4638–4648.
76 Z. Wang, Z. Liu, G. Zhao, Z. Zhang, X. Zhao, X. Wan, Y. Zhang, Z. L. Wang and L. Li, *ACS Nano*, 2022, **16**, 1661–1670.
77 B. Oh, Y. S. Lim, K. W. Ko, H. Seo, D. J. Kim, D. Kong, J. M. You, H. Kim, T. S. Kim, S. Park, D. S. Kwon, J. C. Na, W. K. Han, S. M. Park and S. Park, *Biosens. Bioelectron.*, 2023, **225**, 115060.
78 C. Yang and Z. Suo, *Nat. Rev. Mater.*, 2018, **3**, 125–142.
79 K. K. Kim, I. H. Ha, P. Won, D. G. Seo, K. J. Cho and S. H. Ko, *Nat. Commun.*, 2019, **10**, 2582.
80 T. Qin, X. Li, A. Yang, M. Wu, L. Yu, H. Zeng and L. Han, *Chem. Eng. J.*, 2023, **461**, 141905.
81 H. Zhang, H. Shen, J. Lan, H. Wu, L. Wang and J. Zhou, *Carbohydr. Polym.*, 2022, **295**, 119848.
82 Y. Li, D. Yang, Z. Wu, F. L. Gao, X. Z. Gao, H. Y. Zhao, X. Li and Z. Z. Yu, *Nano Energy*, 2023, **109**, 108324.
83 Z. Hu, J. Li, X. Wei, C. Wang, Y. Cao, Z. Gao, J. Han and Y. Li, *ACS Appl. Mater. Interfaces*, 2022, **14**, 45853–45868.
84 T. Zhu, Y. Ni, G. M. Biesold, Y. Cheng, M. Ge, H. Li, J. Huang, Z. Lin and Y. Lai, *Chem. Soc. Rev.*, 2023, **52**, 473–509.
85 Z. Shen, F. Liu, S. Huang, H. Wang, C. Yang, T. Hang, J. Tao, W. Xia and X. Xie, *Biosens. Bioelectron.*, 2022, **211**, 114298.
86 H. Xie, Q. Yu, J. Mao, S. Wang, Y. Hu and Z. Guo, *J. Mater. Sci.: Mater. Electron.*, 2020, **31**, 10381–10389.
87 W. Zhang, J. Y. Wen, M. G. Ma, M. F. Li, F. Peng and J. Bian, *J. Mater. Res. Technol.*, 2021, **14**, 555–566.
88 Y. Han, L. Sun, C. Wen, Z. Wang, J. Dai and L. Shi, *Biomed. Mater.*, 2022, **17**, 024107.
89 X. Yu, W. Qin, X. Li, Y. Wang, C. Gu, J. Chen and S. Yin, *J. Mater. Chem. A*, 2022, **10**, 15000–15011.
90 H. Yin, S. Li, H. Xie, Y. Wu, X. Zou, Y. Huang and J. Wang, *Colloids Surf., A*, 2022, **642**, 128428.
91 Y. Liu, D. Xu, Y. Ding, X. Lv, T. Huang, B. Yuan, L. Jiang, X. Sun, Y. Yao and J. Tang, *J. Mater. Chem. B*, 2021, **9**, 8862–8870.
92 L. Peng, Y. Su, X. Yang and G. Sui, *J. Colloid Interface Sci.*, 2023, **638**, 313–323.
93 L. Fan, J. Xie, Y. Zheng, D. Wei, D. Yao, J. Zhang and T. Zhang, *ACS Appl. Mater. Interfaces*, 2020, **12**, 22225–22236.
94 G. Chen, J. Huang, J. Gu, S. Peng, X. Xiang, K. Chen, X. Yang, L. Guan, X. Jiang and L. Hou, *J. Mater. Chem. A*, 2020, **8**, 6776–6784.
95 J. Huang, S. Peng, J. Gu, G. Chen, J. Gao, J. Zhang, L. Hou, X. Yang, X. Jiang and L. Guan, *Mater. Horiz.*, 2020, **7**, 2085–2096.
96 A. K. Mondal, S. Wu, D. Xu, Q. Zou, L. Chen, L. Huang, F. Huang and Y. Ni, *Int. J. Biol. Macromol.*, 2021, **187**, 189–199.
97 F. Fu, J. Wang, H. Zeng and J. Yu, *ACS Mater. Lett.*, 2020, **2**, 1287–1301.
98 Z. Qin, X. Sun, Q. Yu, H. Zhang, X. Wu, M. Yao, W. Liu, F. Yao and J. Li, *ACS Appl. Mater. Interfaces*, 2020, **12**, 4944–4953.
99 V. K. Rao, N. Shauloff, X. M. Sui, H. Daniel Wagner, R. Jelinek and R. Jelinek, *J. Mater. Chem. C*, 2020, **8**, 6034–6041.
100 L. Wang, Y. Wang, S. Yang, X. Tao, Y. Zi and W. A. Daoud, *Nano Energy*, 2022, **91**, 106611.
101 Y. Liu, H. Zheng, L. Zhao, S. Liu, K. Yao, D. Li, C. Yiu, S. Gao, R. Avila, P. Chirarattananon, L. Chang, Z. Wang, X. Huang, Z. Xie, Z. Yang and X. Yu, *Research*, 2020, **2020**, 1–11.
102 L. Dong, M. Wang, J. Wu, C. Zhu, J. Shi and H. Morikawa, *ACS Appl. Mater. Interfaces*, 2022, **14**, 9126–9137.
103 X. Dai, Y. Long, B. Jiang, W. Guo, W. Sha, J. Wang, Z. Cong, J. Chen, B. Wang and W. Hu, *Nano Res.*, 2022, **15**, 5461–5468.
104 G. Li, L. Li, P. Zhang, C. Chang, F. Xu and X. Pu, *RSC Adv.*, 2021, **11**, 17437–17444.
105 Y. Luo, M. Yu, Y. Zhang, Y. Wang, L. Long, H. Tan, N. Li, L. Xu and J. Xu, *Nano Energy*, 2022, **104**, 107955.
106 Z. Gao, B. Ren, Z. Fang, H. Kang, J. Han and J. Li, *Sens. Actuators, A*, 2021, **332**, 113121.

107 J. Huang, M. Zhao, Y. Cai, M. Zimniewska, D. Li and Q. Wei, *Adv. Electron. Mater.*, 2020, **6**, 1900934.
108 X. Wang, B. Yang, J. Liu and C. Yang, *J. Mater. Chem. A*, 2017, **5**, 1176–1183.
109 S. G. Yoon, H. J. Koo and S. T. Chang, *ACS Appl. Mater. Interfaces*, 2015, **7**, 27562–27570.
110 J. Mo, Y. Dai, C. Zhang, Y. Zhou, W. Li, Y. Song, C. Wu and Z. Wang, *Mater. Horiz.*, 2021, **8**, 3409–3416.
111 H. Wang, J. Xu, K. Li, Y. Dong, Z. Du and S. Wang, *J. Mater. Chem. B*, 2022, **10**, 1301–1307.
112 O. Hu, J. Lu, S. Weng, L. Hou, X. Zhang and X. Jiang, *Polymer*, 2022, **254**, 125109.
113 Z. Ling, J. Ma, S. Zhang, L. Shao, C. Wang and J. Ma, *Int. J. Biol. Macromol.*, 2022, **216**, 193–202.
114 X. Sun, Y. Liang, L. Ye and H. Liang, *J. Mater. Chem. B*, 2021, **9**, 7751–7759.
115 J. Y. Sun, X. Zhao, W. R. K. Illeperuma, O. Chaudhuri, K. H. Oh, D. J. Mooney, J. J. Vlassak and Z. Suo, *Nature*, 2012, **489**, 133–136.
116 Y. Liang, L. Ye, X. Sun, Q. Lv and H. Liang, *ACS Appl. Mater. Interfaces*, 2020, **12**, 1577–1587.
117 R. Chen, X. Xu, D. Yu, C. Xiao, M. Liu, J. Huang, T. Mao, C. Zheng, Z. Wang and X. Wu, *J. Mater. Chem. C*, 2018, **6**, 11193–11201.
118 Z. Deng, B. Lin, W. Wang, L. Bai, H. Chen, L. Yang, H. Yang and D. Wei, *Int. J. Biol. Macromol.*, 2021, **191**, 627–636.
119 S. Liu and L. Li, *ACS Appl. Mater. Interfaces*, 2017, **9**, 26429–26437.
120 X. Zhang, X. Yang, Q. Dai, Y. Zhang, H. Pan, C. Yu, Q. Feng, S. Zhu, H. Dong and X. Cao, *J. Mater. Chem. B*, 2021, **9**, 176–186.
121 C. Hu, Y. Zhang, X. Wang, L. Xing, L. Shi and R. Ran, *ACS Appl. Mater. Interfaces*, 2018, **10**, 44000–44010.
122 J. Yin, S. Pan, L. Wu, L. Tan, D. Chen, S. Huang, Y. Zhang and P. He, *J. Mater. Chem. C*, 2020, **8**, 17349–17364.
123 Z. He and W. Yuan, *ACS Appl. Mater. Interfaces*, 2021, **13**, 1474–1485.
124 Q. Li, J. Chen, Y. Zhang, C. Chi, G. Dong, J. Lin and Q. Chen, *ACS Appl. Mater. Interfaces*, 2021, **13**, 51546–51555.
125 Y. Wang, S. Liu, Q. Wang, X. Ji, X. An, H. Liu and Y. Ni, *Int. J. Biol. Macromol.*, 2022, **205**, 442–451.
126 C. Liu, R. Zhang, P. Li, J. Qu, P. Chao, Z. Mo, T. Yang, N. Qing and L. Tang, *ACS Appl. Mater. Interfaces*, 2022, **14**, 26088–26098.
127 X. X. Zhang, J. Cao, Y. Yang, X. Wu, Z. Zheng and X. X. Zhang, *Chem. Eng. J.*, 2019, **374**, 730–737.
128 J. Liu, H. Wang, R. Ou, X. Yi, T. Liu, Z. Liu and Q. Wang, *Chem. Eng. J.*, 2021, **426**, 130722.
129 C. Luo, A. Guo, Y. Zhao, J. Sun and Z. Li, *Mater. Today Commun.*, 2021, **27**, 102375.
130 F. He, X. You, H. Gong, Y. Yang, T. Bai, W. Wang, W. Guo, X. Liu and M. Ye, *ACS Appl. Mater. Interfaces*, 2020, **12**, 6442–6450.
131 Q. Wang, X. Pan, C. Lin, D. Lin, Y. Ni, L. Chen, L. Huang, S. Cao and X. Ma, *Chem. Eng. J.*, 2019, **370**, 1039–1047.
132 X. Sui, H. Guo, C. Cai, Q. Li, C. Wen, X. Zhang, X. Wang, J. Yang and L. Zhang, *Chem. Eng. J.*, 2021, **419**, 129478.
133 L. Zhao, T. Ke, Q. Ling, J. Liu, Z. Li and H. Gu, *ACS Appl. Polym. Mater.*, 2021, **3**, 5494–5508.
134 J. Zou, X. Jing, Z. Chen, S.-J. Wang, X.-S. Hu, P.-Y. Feng, Y.-J. Liu, J. Zou, X. Jing, Z. Chen, S.-J. Wang, X.-S. Hu, P.-Y. Feng and Y.-J. Liu, *Adv. Funct. Mater.*, 2023, **33**, 2213895.
135 J. Wang, F. Tang, C. Yao, L. Li, J. Wang, F. Tang, L. Li and C. Yao, *Adv. Funct. Mater.*, 2023, 2214935.
136 J. Liu, X. Chen, B. Sun, H. Guo, Y. Guo, S. Zhang, R. Tao, Q. Yang and J. Tang, *J. Mater. Chem. A*, 2022, **10**, 25564–25574.
137 A. R. Angumeenal and D. Venkappayya, *LWT–Food Sci. Technol.*, 2013, **50**, 367–370.
138 G. S. Dhillon, S. K. Brar, M. Verma and R. D. Tyagi, *Food Bioprocess Technol.*, 2010, **44**(4), 505–529.
139 N. Sarwar, U. Bin Humayoun, M. Kumar, S. F. A. Zaidi, J. H. Yoo, N. Ali, D. I. Jeong, J. H. Lee and D. H. Yoon, *J. Clean. Prod.*, 2021, **292**, 125974.
140 R. Reena, R. Sindhu, P. Athiyaman Balakumaran, A. Pandey, M. K. Awasthi and P. Binod, *Fuel*, 2022, **327**, 125181.
141 A. Amato, A. Becci and F. Beolchini, *Crit. Rev. Biotechnol.*, 2020, **40**, 199–212.
142 B. C. Behera, R. Mishra and S. Mohapatra, *Food Front.*, 2021, **2**, 62–76.
143 P. L. Show, K. O. Oladele, Q. Y. Siew, F. A. Aziz Zakry, J. C. W. Lan and T. C. Ling, *Front. Life Sci.*, 2015, **8**, 271–283.
144 P. Z. de Oliveira, L. P. de Souza Vandenberghe, C. Rodrigues, G. V. de Melo Pereira and C. R. Soccol, *Process Biochem.*, 2022, **113**, 107–112.
145 A. Bodaghi, M. Adeli, A. Dadkhahtehrani and Z. Tu, *J. Mol. Liq.*, 2017, **242**, 53–58.
146 S. Wang, C. Xu, S. Yu, X. Wu, Z. Jie and H. Dai, *J. Mech. Behav. Biomed. Mater.*, 2019, **94**, 42–50.
147 J. Yang, A. R. Webb and G. A. Ameer, *Adv. Mater.*, 2004, **16**, 511–516.
148 T. Taguchi, H. Saito, H. Aoki, Y. Uchida, M. Sakane, H. Kobayashi and J. Tanaka, *Mater. Sci. Eng., C*, 2006, **26**, 9–13.
149 K. A. Uyanga, O. P. Okpozo, O. S. Onyekwere and W. A. Daoud, *React. Funct. Polym.*, 2020, **154**, 104682.
150 M. G. Raucci, M. A. Alvarez-Perez, C. Demitri, D. Giugliano, V. De Benedictis, A. Sannino and L. Ambrosio, *J. Biomed. Mater. Res., Part A*, 2015, **103**, 2045–2056.
151 M. Baumgartner, F. Hartmann, M. Drack, D. Preninger, D. Wirthl, R. Gerstmayr, L. Lehner, G. Mao, R. Pruckner, S. Demchyshyn, L. Reiter, M. Strobel, T. Stockinger, D. Schiller, S. Kimeswenger, F. Greibich, G. Buchberger, E. Bradt, S. Hild, S. Bauer and M. Kaltenbrunner, *Nat. Mater.*, 2020, **19**, 1102–1109.
152 Z. Li, X. Meng, W. Xu, S. Zhang, J. Ouyang, Z. Zhang, Y. Liu, Y. Niu, S. Ma, Z. Xue, A. Song, S. Zhang and C. Ren, *Soft Matter*, 2020, **16**, 7323–7331.
153 Z. Zhang, S. Lu, R. Cai and W. Tan, *Nano Today*, 2021, **38**, 101202.
154 C. Xu, Z. Zheng, M. Lin, Q. Shen, X. Wang, B. Lin and L. Fu, *ACS Appl. Mater. Interfaces*, 2020, **12**, 35482–35492.

155 L. Chen, X. Chang, H. Wang, J. Chen and Y. Zhu, *Nano Energy*, 2022, **96**, 107077.
156 Q. Wang, X. Pan, H. Zhang, S. Cao, X. Ma, L. Huang, L. Chen and Y. Ni, *J. Mater. Chem. A*, 2021, **9**, 3968–3975.
157 J. Krasensky and C. Jonak, *J. Exp. Bot.*, 2012, **63**, 1593–1608.
158 M. Mohammadzadeh, M. Honarvar, A. R. Zarei, M. Mashhadi Akbar Boojar and H. Bakhoda, *J. Food Sci. Technol.*, 2018, **55**, 1215–1223.
159 L. Rivoira, S. Studzińska, M. Szultka-Młyńska, M. C. Bruzzoniti and B. Buszewski, *Anal. Bioanal. Chem.*, 2017, **409**, 5133–5141.
160 A. Siddique, G. Kandpal and P. Kumar, *J. Pure Appl. Microbiol.*, 2018, **12**, 1655–1659.
161 P. M. F. Teymoori, G. Asghari, H. Farhadnejad, M. Nazarzadeh, M. Atifeh and F. Azizi, *Int. J. Food Sci. Nutr.*, 2019, **71**, 332–340.
162 E. Karna, L. Szoka, T. Y. L. Huynh and J. A. Palka, *Cell. Mol. Life Sci.*, 2020, **77**, 1911–1918.
163 J. Yang, X. Sui, Q. Li, W. Zhao, J. Zhang, Y. Zhu, P. Chen and L. Zhang, *ACS Biomater. Sci. Eng.*, 2019, **5**, 2621–2630.
164 M. P. Hwang, X. Ding, J. Gao, A. P. Acharya, S. R. Little and Y. Wang, *Soft Matter*, 2018, **14**, 387–395.
165 J. Sun, F. Zeng, H. Jian and S. Wu, *Biomacromolecules*, 2013, **14**, 728–736.
166 X. Qu, S. Wang, Y. Zhao, H. Huang, Q. Wang, J. Shao, W. Wang and X. Dong, *Chem. Eng. J.*, 2021, **425**, 131523.
167 L. Wang, T. Shan, B. Xie, C. Ling, S. Shao, P. Jin and Y. Zheng, *Food Chem.*, 2019, **272**, 530–538.
168 F. Zulfiqar, N. A. Akram and M. Ashraf, *Planta*, 2019, **251**, 1–17.
169 A. L. Furlan, E. Bianucci, W. Giordano, S. Castro and D. F. Becker, *Plant Physiol. Biochem.*, 2020, **151**, 566–578.
170 X. Liang, L. Zhang, S. K. Natarajan and D. F. Becker, *Antioxid. Redox Signaling*, 2013, **19**, 998–1011.
171 S. Kishitani, K. Watanabe, S. Yasuda, K. Arakawa and T. Takabe, *Plant, Cell Environ.*, 1994, **17**, 89–95.
172 L. Cao, Z. Zhao, X. Wang, X. Huang, J. Li and Y. Wei, *Adv. Mater. Technol.*, 2022, **7**, 2101382.
173 Z. Zhang, Z. Zheng, Y. Zhao, J. Hu and H. Wang, *Compos. Sci. Technol.*, 2021, **213**, 108968.
174 J. Wang, Y. Deng, Z. Ma, Y. Wang, S. Zhang and L. Yan, *Green Chem.*, 2021, **23**, 5120–5128.
175 Z. Guo, W. Liu and A. Tang, *Eur. Polym. J.*, 2022, **164**, 110977.
176 Q. Fan, Y. Nie, Q. Sun, W. Wang, L. Bai, H. Chen, L. Yang, H. Yang and D. Wei, *ACS Appl. Polym. Mater.*, 2022, **4**, 1626–1635.
177 E. Feng, J. Li, G. Zheng, X. Li, J. Wei, Z. Wu, X. Ma and Z. Yang, *Chem. Eng. J.*, 2022, **432**, 134406.
178 E. Feng, G. Zheng, X. Li, M. Zhang, X. Li, X. Han, L. Cao and Z. Wu, *Colloids Surf., A*, 2023, **656**, 130390.
179 Y. Du, Y. Sun, S. Lu, K. Zhang, C. Song, B. Li, X. He and Q. Li, *J. Polym. Sci.*, 2022, **60**, 2733–2740.
180 G. Sathishkumar, K. Gopinath, K. Zhang, E. T. Kang, L. Xu and Y. Yu, *J. Mater. Chem. B*, 2022, **10**, 2296–2315.
181 H. Jafari, P. Ghaffari-Bohlouli, S. V. Niknezhad, A. Abedi, Z. Izadifar, R. Mohammadinejad, R. S. Varma and A. Shavandi, *J. Mater. Chem. B*, 2022, **10**, 5873–5912.
182 P. B. D. Firda, Y. T. Malik, J. K. Oh, E. K. Wujcik and J. W. Jeon, *Polymers*, 2021, **13**, 2992.
183 N. Saracogullari, D. Gundogdu, F. N. Ozdemir, Y. Soyer and I. Erel-Goktepe, *Colloids Surf., A*, 2021, **617**, 126313.
184 P. L. de Hoyos-Martínez, J. Merle, J. Labidi and F. Charrier-El Bouhtoury, *J. Clean. Prod.*, 2019, **206**, 1138–1155.
185 N. F. Sukor, V. P. Selvam, R. Jusoh, N. S. Kamarudin and S. A. Rahim, *J. Food Eng.*, 2021, **296**, 110437.
186 H. Zheng, N. Lin, Y. He and B. Zuo, *ACS Appl. Mater. Interfaces*, 2021, **13**, 40013–40031.
187 H. Zheng, M. Chen, Y. Sun and B. Zuo, *Chem. Eng. J.*, 2022, **446**, 136931.
188 H. Bai, Z. Zhang, Y. Huo, Y. Shen, M. Qin and W. Feng, *J. Mater. Sci. Technol.*, 2022, **98**, 169–176.
189 F. B. Kadumudi, M. Hasany, M. K. Pierchala, M. Jahanshahi, N. Taebnia, M. Mehrali, C. F. Mitu, M. A. Shahbazi, T. G. Zsurzsan, A. Knott, T. L. Andresen and A. Dolatshahi-Pirouz, *Adv. Mater.*, 2021, **33**, 2100047.
190 X. X. Wang, X. X. Wang, J. Yin, N. Li, Z. Zhang, Y. Xu, L. Zhang, Z. Qin and T. Jiao, *Composites, Part B*, 2022, **241**, 110052.
191 B. Kang, X. Yan, Z. Zhao and S. Song, *Langmuir*, 2022, **38**, 7013–7023.
192 X. Zhang, K. Liu, M. Qin, W. Lan, L. Wang, Z. Liang, X. Li, Y. Wei, Y. Hu, L. Zhao, X. Lian and D. Huang, *Carbohydr. Polym.*, 2023, **309**, 120702.
193 C. Shao, L. Meng, C. Cui and J. Yang, *J. Mater. Chem. C*, 2019, **7**, 15208–15218.
194 C. Cui, C. Shao, L. Meng and J. Yang, *ACS Appl. Mater. Interfaces*, 2019, **11**, 39228–39237.
195 D. K. Patel, K. Ganguly, S. D. Dutta, T. V. Patil, A. Randhawa and K. T. Lim, *Int. J. Biol. Macromol.*, 2023, **229**, 105–122.
196 X. Gong, C. Fu, N. Alam, Y. Ni, L. Chen, L. Huang and H. C. Hu, *Ind. Crops Prod.*, 2022, **176**, 114412.
197 X. Gong, C. Fu, N. Alam, Y. Ni, L. Chen, L. Huang and H. Hu, *Biomacromolecules*, 2022, **23**, 2272–2279.
198 S. Hao, C. Shao, L. Meng, C. Cui, F. Xu and J. Yang, *ACS Appl. Mater. Interfaces*, 2020, **12**, 56509–56521.
199 F. Wang, C. Chen, J. Wang, Z. Xu, F. Shi and N. Chen, *Colloids Surf., A*, 2023, **658**, 130591.
200 J. Lu, X. Han, L. Dai, C. Li, J. Wang, Y. Zhong, F. Yu and C. Si, *Carbohydr. Polym.*, 2020, **250**, 117010.
201 X. Liu, Y. Ma, X. Zhang and J. Huang, *Colloids Surf., A*, 2021, **613**, 126076.
202 K. Chen, F. Wang, Y. Hu, M. Liu, P. Liu, Y. Yu, Q. Feng and X. Xiao, *ACS Appl. Polym. Mater.*, 2022, **4**, 2036–2046.
203 P. He, J. Wu, X. Pan, L. Chen, K. Liu, H. Gao, H. Wu, S. Cao, L. Huang and Y. Ni, *J. Mater. Chem. A*, 2020, **8**, 3109–3118.
204 X. Pan, Q. Wang, R. Guo, Y. Ni, K. Liu, X. Ouyang, L. Chen, L. Huang, S. Cao and M. Xie, *J. Mater. Chem. A*, 2019, **7**, 4525–4535.
205 H. Lei, J. Zhao, X. Ma, H. Li and D. Fan, *Adv. Healthcare Mater.*, 2021, **10**, 2101089.

206 X. X. Liu, J. Qin, J. Wang, Y. Chen, G. Miao, P. Qi, J. Qu, J. Zheng and X. X. Liu, *Colloids Surf., A*, 2022, **632**, 127823.
207 Q. Yan, M. Zhou and H. Fu, *Composites, Part B*, 2020, **201**, 108356.
208 S. Wang, H. Cheng, B. Yao, H. He, L. Zhang, S. Yue, Z. Wang and J. Ouyang, *ACS Appl. Mater. Interfaces*, 2021, **13**, 20735–20745.
209 H. Qiao, P. Qi, X. Zhang, L. Wang, Y. Tan, Z. Luan, Y. Xia, Y. Li and K. Sui, *ACS Appl. Mater. Interfaces*, 2019, **11**, 7755–7763.
210 A. Kumar, B. Singh, P. Raigond, C. Sahu, U. N. Mishra, S. Sharma and M. K. Lal, *Food Res. Int.*, 2021, **142**, 110193.
211 Y. Y. Gao, C. Deng, Y. Y. Du, S. C. Huang and Y. Z. Wang, *Polym. Degrad. Stab.*, 2019, **161**, 298–308.
212 A. Paula, M. Bloot, D. Lahis Kalschne, J. Andrêa, S. Amaral, J. Baraldi and C. Canan, *Food Rev. Int.*, 2021, 1–20.
213 L. Gillberg and B. Ternell, *J. Food Sci.*, 1976, **41**, 1070–1075.
214 P. Åman and L. Gillberg, *J. Food Sci.*, 1977, **42**, 1114–1116.
215 H. Ren, T. Li, H. Wan and J. Yue, *Resour. Technol.*, 2017, **3**, 226–231.
216 L. Shao, Y. Li, Z. Ma, Y. Bai, J. Wang, P. Zeng, P. Gong, F. Shi, Z. Ji, Y. Qiao, R. Xu, J. Xu, G. Zhang, C. Wang and J. Ma, *ACS Appl. Mater. Interfaces*, 2020, **12**, 26496–26508.
217 S. Zhang, Y. Zhang, B. Li, P. Zhang, L. Kan, G. Wang, H. Wei, X. Zhang and N. Ma, *ACS Appl. Mater. Interfaces*, 2019, **11**, 32441–32448.
218 Y. Nie, D. Yue, W. Xiao, W. Wang, H. Chen, L. Bai, L. Yang, H. Yang and D. Wei, *Chem. Eng. J.*, 2022, **436**, 135243.
219 C. Lu, J. Qiu, M. Sun, Q. Liu, E. Sakai and G. Zhang, *Cellulose*, 2021, **28**, 4253–4265.
220 J. Xiang, S. Yang, J. Zhang, J. Wu, Y. Shao, Z. Wang and M. Yang, *Polym. Bull.*, 2022, **79**, 2667–2684.
221 L. Ugarte, S. Gómez-Fernández, C. Peña-Rodríuez, A. Prociak, M. A. Corcuera and A. Eceiza, *ACS Sustainable Chem. Eng.*, 2015, **3**, 3382–3387.
222 M. L. Manca, S. Mir-Palomo, C. Caddeo, A. Nacher, O. Díez-Sales, J. E. Peris, J. L. Pedraz, A. M. Fadda and M. Manconi, *Int. J. Pharm.*, 2019, **555**, 175–183.
223 Y. Wang, J. Chen, J. Tian, G. Wang, W. Luo, Z. Huang, Y. Huang, N. Li, M. Guo and X. Fan, *J. Nanobiotechnol.*, 2022, **20**, 1–16.
224 D. Govindaraj, M. Rajan, M. A. Munusamy, M. D. Balakumaran and P. T. Kalaichelvan, *RSC Adv.*, 2015, **5**, 44705–44713.
225 Y. Wu, J. Qu, X. Zhang, K. Ao, Z. Zhou, Z. Zheng, Y. Mu, X. Wu, Y. Luo and S. P. Feng, *ACS Nano*, 2021, **15**, 13427–13435.
226 Z. Li, F. Yin, W. He, T. Hang, Z. Li, J. Zheng, X. Li, S. Jiang and Y. Chen, *Int. J. Biol. Macromol.*, 2023, **230**, 123117.
227 C. A. G. Quispe, C. J. R. Coronado and J. A. Carvalho, *Renewable Sustainable Energy Rev.*, 2013, **27**, 475–493.
228 H. W. Tan, A. R. Abdul Aziz and M. K. Aroua, *Renewable Sustainable Energy Rev.*, 2013, **27**, 118–127.
229 B. R. Bewley, A. Berkaliev, H. Henriksen, D. B. Ball and L. S. Ott, *Fuel Process. Technol.*, 2015, **138**, 419–423.
230 M. Ayoub and A. Z. Abdullah, *Renewable Sustainable Energy Rev.*, 2012, **16**, 2671–2686.
231 I. Karageorgou, S. Grigorakis, S. Lalas and D. P. Makris, *Eur. Food Res. Technol.*, 2017, **243**, 1839–1848.
232 E. Mouratoglou, V. Malliou and D. P. Makris, *Waste Biomass Valorization*, 2016, **7**, 1377–1387.
233 Z. Zhao, J. Jiang, M. Zheng and F. Wang, *Chem. Eng. J.*, 2021, **411**, 128516.
234 A. D. Shejale and G. D. Yadav, *Int. J. Hydrogen Energy*, 2021, **46**, 4808–4826.
235 B. Xiao, M. Zheng, J. Pang, Y. Jiang, H. Wang, R. Sun, A. Wang, X. Wang and T. Zhang, *Ind. Eng. Chem. Res.*, 2015, **54**, 5862–5869.
236 M. Nassiri Asl and H. Hosseinzadeh, *Phyther. Res.*, 2008, **22**, 709–724.
237 L. A. Baltina, R. M. Kondratenko, L. A. Baltina, O. A. Plyasunova, A. G. Pokrovskii and G. A. Tolstikov, *Pharm. Chem. J.*, 2010, **43**, 539–548.
238 O. Y. Selyutina and N. E. Polyakov, *Int. J. Pharm.*, 2019, **559**, 271–279.
239 J. Li, H. Cao, P. Liu and G. Cheng, *BioMed Res. Int.*, 2014, **2014**, 15.
240 G. Cirillo, M. Curcio, O. I. Parisi, F. Puoci, F. Iemma, U. G. Spizzirri, D. Restuccia and N. Picci, *Food Chem.*, 2011, **125**, 1058–1063.
241 T. Charpe and V. R. Process, *Chem. Eng. Process.*, 2012, **54**, 37–41.
242 H. Zhang, N. Tang, X. Yu, Z. Guo, Z. Liu, X. Sun, M. H. Li and J. Hu, *Chem. Eng. J.*, 2022, **430**, 132779.
243 K.-I. Kim, S. Lee, X. Jin, S. Ji Kim, K. Jo, J. Heon Lee, K. I. Kim, J. H. Lee, S. Lee, X. Jin, K. Jo and S. J. Kim, *Small*, 2017, **13**, 1601926.
244 S. Kannappan, J. Chang, P. R. Sundharbaabu, J. H. Heo, W. kee Sung, J. C. Ro, K. K. Kim, J. B. B. Rayappan and J. H. Lee, *BioChip J.*, 2022, **16**, 490–500.
245 X. Jin, S. Kannappan, N. D. Hapsari, Y. Jin, K. K. Kim, J. H. Lee and K. Jo, *Small Struct.*, 2023, 2200361.
246 Y. W. Kwon, C. H. Lee, D. H. Choi and J. Il Jin, *J. Mater. Chem.*, 2009, **19**, 1353–1380.
247 A. Jain, G. Wang and K. M. Vasquez, *Biochimie*, 2008, **90**, 1117–1130.
248 A. Carré, V. Lacarrière and W. Birch, *J. Colloid Interface Sci.*, 2003, **260**, 49–55.
249 H. R. Dash and S. Das, *Mol. Biotechnol.*, 2017, **60**, 141–153.
250 P. H. Nimbkar and V. D. Bhatt, *Forensic Sci. Int.*, 2022, **336**, 111352.
251 J. Pawlowski and E. Al, *Sci. Total Environ.*, 2022, **818**, 151783.
252 S. C. Y. Ip, S. wah Lin and K. ming Lai, *Sci. Justice*, 2015, **55**, 200–208.
253 *DNA and RNA Molecular Weights and Conversions|Thermo Fisher Scientific – KR*, **https://www.thermofisher.com/kr/ko/home/references/ambion-tech-support/rna-tools-and-calculators/dna-and-rna-molecular-weights-and-conversions.html**, accessed 15 March 2023.
254 X. Zhang, D. Wang, H. Liu, L. Yue, Y. Bai and J. He, *Eur. Polym. J.*, 2020, **133**, 109741.
255 B. Kang, X. Yan, H. Tang, Z. Zhao and S. Song, *ACS Appl. Polym. Mater.*, 2022, **4**, 1159–1172.

256 B. Chen, W. Wang, X. Yan, S. Li, S. Jiang, S. Liu, X. Ma and X. Yu, *Chem.–Eur. J.*, 2020, **26**, 11604–11613.
257 Q. Zhang, X. Liu, L. Duan and G. Gao, *J. Mater. Chem. A*, 2021, **9**, 1835–1844.
258 J. Wyman, *Chem. Rev.*, 1936, **19**, 213–239.
259 R. Govrin, S. Tcherner, T. Obstbaum and U. Sivan, *J. Am. Chem. Soc.*, 2018, **140**, 14206–14210.
260 A. G. Morena, A. Bassegoda, M. Natan, G. Jacobi, E. Banin and T. Tzanov, *ACS Appl. Mater. Interfaces*, 2022, **14**, 37270–37279.
261 H. Akiyama, K. Fujii, O. Yamasaki, T. Oono and K. Iwatsuki, *J. Antimicrob. Chemother.*, 2001, **48**, 487–491.
262 Y. Wang, S. Liu, K. Ding, Y. Zhang, X. Ding and J. Mi, *J. Mater. Chem. B*, 2021, **9**, 4746–4762.
263 F. Weber, E. Sagstuen, Q. Z. Zhong, T. Zheng and H. Tiainen, *ACS Appl. Mater. Interfaces*, 2020, **12**, 52457–52466.
264 M. Wang, H. Zhou, H. Du, L. Chen, G. Zhao, H. Liu, X. Jin, W. Chen and A. Ma, *Chem. Eng. J.*, 2022, **446**, 137163.
265 R. Hu, G. Ji, J. Zhao, X. Gu, L. Zhou and J. Zheng, *Compos. Sci. Technol.*, 2022, **217**, 109110.
266 Z. Wang, H. Zhou, W. Chen, Q. Li, B. Yan, X. Jin, A. Ma, H. Liu and W. Zhao, *ACS Appl. Mater. Interfaces*, 2018, **10**, 14045–14054.
267 Z. Wang, H. Zhou, J. Lai, B. Yan, H. Liu, X. Jin, A. Ma, G. Zhang, W. Zhao and W. Chen, *J. Mater. Chem. C*, 2018, **6**, 9200–9207.
268 Z. Wang, Z. Ma, S. Wang, M. Pi, X. Wang, M. Li, H. Lu, W. Cui and R. Ran, *Carbohydr. Polym.*, 2022, **298**, 120128.
269 E. J. Brettrager, S. M. Cuya, Z. E. Tibbs, J. Zhang, C. N. Falany, S. G. Aller and R. C. A. M. van Waardenburg, *Sci. Rep.*, 2023, **13**, 1–12.
270 N. S. Clovis, P. Alam, A. K. Chand, D. Sardana, M. F. Khan and S. Sen, *J. Photochem. Photobiol., A*, 2023, **437**, 114432.
271 Y. Gao, S. Gu, F. Jia and G. Gao, *J. Mater. Chem. A*, 2020, **8**, 24175–24183.
272 L. Y. Hsiao, L. Jing, K. Li, H. Yang, Y. Li and P. Y. Chen, *Carbon*, 2020, **161**, 784–793.